Research and Development

UCRL-11984

UNIVERSITY OF CALIFORNIA

Lawrence Radiation Laboratory
Berkeley, California

AEC Contract No. W-7405-eng-48

MAGNETIC PROPERTIES OF CURIUM METAL AND ITS COMPOUNDS

Sayed A. Marei

(Ph.D. Thesis)

May 18, 1965

MAGNETIC PROPERTIES OF CURIUM METAL AND ITS COMPOUNDS

Contents

Abstract iii

I. Introduction 1

II. Magnetic Susceptibility Measurements

A. Principle of the Apparatus 2

B. Apparatus Calibration 6

C. Calculation of Parameters 7

III. Operation of Magnetic Susceptibility Apparatus

A. Preparation of Suspension Fibers 13

B. Preparation of Sample Tubes 17

C. Loading the Apparatus 20

D. Observing the Sample and Adjusting its Position 22

E. Making Deflection Measurements 22

F. Unloading the Sample 22

IV. Preparation of Materials

A. Preparation of Curium Metal 23

B. Preparation of Curium Trifluoride 37

C. Preparation of Curium Oxychloride 37

Curium Trifluoride in Lanthanum Trifluoride Matrix 42

V. Results

A. Curium Metal 44

B. Curium Trifluoride 62

C. Curium Oxychloride 64

D. Curium - Lanthanum Mixture 71

VI. Discussion 81

Acknowledgments 94

References 97

MAGNETIC PROPERTIES OF CURIUM METAL AND ITS COMPOUNDS

Sayed A. Marei
Department of Chemistry and Lawrence Radiation Laboratory
University of California
Berkeley, California

May 18, 1965

ABSTRACT

The magnetic susceptibility of curium metal has been measured from -253 to 250°C. The metal followed Curie-Weiss law above liquid nitrogen temperature up to the temperature studied. The effective magnetic moment for the metal was found to be 7.99±0.15 indicating the presence of $5f^7$ configuration in the metal. No magnetic transition was observed in the temperature range studied.

The magnetic susceptibility of Cm^{+3} in curium trifluoride, curium oxychloride, and 5.6 mole percent curium trifluoride diluted with lanthanum trifluoride has been measured. The effective moment for Cm^{+3} was found to be 7.65±0.1 Bohr magneton, giving a Landé g factor of 1.93±0.03, pointing toward an appreciable departure from Russell-Saunders coupling. The molecular field constant Δ was found to be small and decreasing with increasing magnetic dilution. The following Δ values were found for curium compounds.

Compound	Δ^{o}
CmOCl	23±3
$CmF_3 \cdot 1/2\ H_2O$	5±3
5.6% CmF_3	5±3

I. INTRODUCTION

Extensive studies are being made to elucidate the nature of the metallic bond in the heavy-element region. In comparison with the more common metals, the heavy metals-uranium, neptunium, and plutonium-all exhibit anomalous physical properties. For example they have quite complex room temperature crystal structures instead of the simple ones (hexagonal close-packed, face-centered cubic, or body-centered cubic) found in most metals. They have anomalous magnetic and electrical properties. Americium metal was prepared and investigated[1,2] by McWhan. It was found to be a rare-earth-like metal.

Until very recently almost no work was reported about curium metal. Cunningham and Wallmann[3] prepared curium metal using methods similar to those used for preparing americium metal. They reported the crystal structure of curium metal as double hexagonal close-packed, dhcp ($a=3.496 \pm 0.003A^{o}$, $c = 11.331 \pm 0.005A^{o}$) similar to that of americium and the early members of the rare-earth series. The melting point of the metal was observed to be $1340 \pm 40^{o}C$. No magnetic measurements were reported in the literature about curium metal. The only magnetic measurements reported about curium are those of Crane et al.[4,5]. They measured the magnetic susceptibility of curium trifluoride and reported the molar susceptibility of $22,500 \pm 4000$ c.g.s. at $295^{o}K$ and $58,000 \pm 6000$ c.g.s. at $77^{o}K$. They also measured the molar magnetic susceptibility of solid CmF_3 in 10 mole percent in solid LaF_3 and found the value to be $26,000 \pm 700 \times 10^{-6}$ c.g.s. units at $296^{o}K$. The experimental error in Crane's measurements was rather great. He used Cm^{242} for these measurements; therefore, the temperature of the samples was probably significantly higher than that of the environment, because of the self-heating caused by the radioactivity of the isotope Cm^{242} (half-life = 163 days with specific activity of 3.7×10^{9} c/p/m/ug. assuming 50% geometry).

In the following work the methods for preparing pure, well crystallized metal are discussed in detail. The magnetic susceptibility of the metal has been measured from -196 to $550^{o}C$. The description of a new apparatus (for extending the measurements to liquid hydrogen and liquid helium temperatures) is given.

The magnetic susceptibility of Cm^{+3} was measured in several curium compounds, over a wide range of temperature. The results found are discussed in the light of the properties of the other actinide and rare earth elements.

II. MAGNETIC SUSCEPTIBILITY MEASUREMENTS

Cunningham[6] has described an apparatus used to measure the magnetic susceptibility of submicrogram quantities of the plus three ions of berkelium and californium. This apparatus was modified[2] to measure the susceptibility of americium metal, curium metal, and their compounds.

A. Principle of the Apparatus

The susceptibility is measured by a modified Faraday method in which the sample, suspended on a long quartz fiber, is exposed to an inhomogeneous magnetic field. The principle of this apparatus is sketched in Fig. 1. The fiber is of uniform cross-section and is assumed to be infinitely flexible. The sample is suspended midway between the pole faces of the magnet, which are shaped in such a way that the field gradient in the vicinity of the sample is large in the xy plane and negligible in the z direction. The sample experiences a force F_1 in the x direction and a gravitional force F_2, normal to F_1. An additional force F_3, acts on the center of mass of the suspension fiber. (The magnetic force on the fiber is too small to be considered.)

At equilibrium, the sum of the moments of force acting about the pivot P is zero. So at equilibrium the following relation is valid,

$$F_2\ d + F_3\ d/2 = F_1\ L\ \mathrm{Cos}\theta \qquad (1)$$

where d is the linear displacement of the sample due to the magnetic force and L is the length of the fiber, $F_2 = m_s g$ where m_s mass of the sample, and g is the acceleration of gravity; $F_3 = m_f g$ where m_f mass of the fiber. $F_1 = m_s\ \chi_{sg}\ H\ \partial H/\partial x$ where χ_{sg} is the gram susceptibility of the sample, H is the magnetic field at the sample and $H\ \partial H/\partial x$ is the field

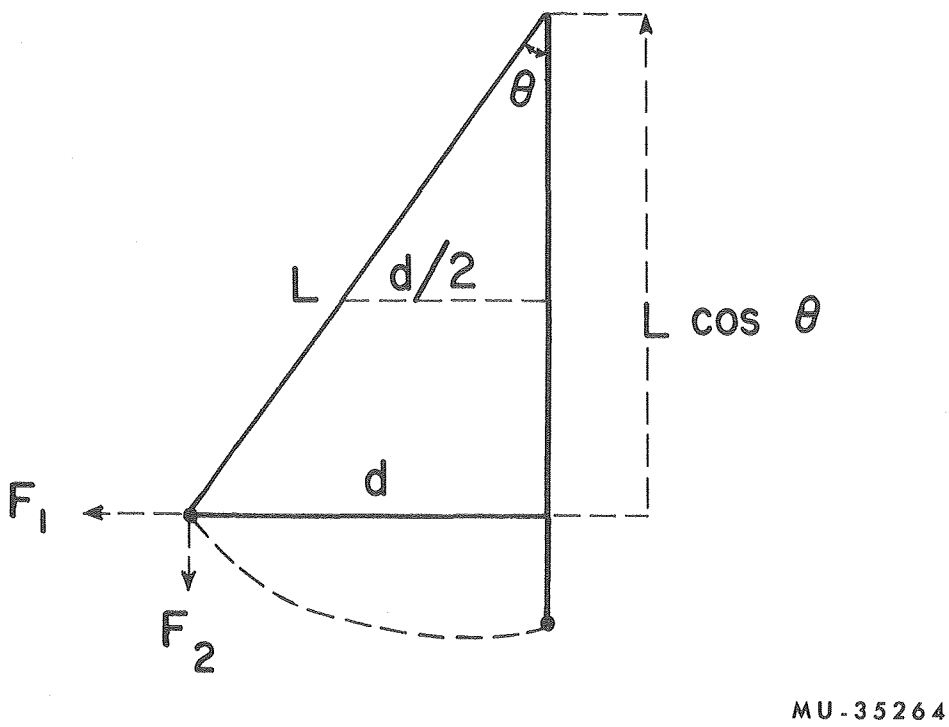

Fig. 1. Principle of magnetic susceptibility apparatus.

gradient in the x direction. (The pole pieces are shaped to produce as large a volume of uniform $H\partial H/\partial x$ about the sample as possible, but in practice it is difficult to secure satisfactory constancy even in a volume as small as one mm^3. Hence it is customary to restore the sample with the magnet current on to the same position in space that it occupied with the current off, by a micro meter-controlled compensating shift of the suspension point P.) Substituting for F_1, F_2, F_3, their corresponding values gives

$$(m_s + m_f)\ gd = m_s\ \chi_{sg}\ H \frac{\partial H}{\partial x} L \cos\Theta \qquad (2)$$

If θ is small, as is usually the case experimentally so that $\cos\theta$ may be taken as unity (for the maximum deflection obtained in these measurements θ was 0.33° for which $\cos\theta = 0.99998$) then,

$$(m_s + m_{f/2})\ g\ d = m_s\ \chi_{sg}\ H \frac{\partial H}{\partial x} L \qquad (3)$$

$$d = m_s\ \chi_{sg}\ \frac{H\ \partial H}{\partial x} L\ /\ (m_s + m_{f/2})\ g \qquad (4)$$

equation (4) may be rearranged to give

$$\chi_{sg} = (m_s + m_{f/2})\ d\ g\ /\ m_s\ H \frac{\partial H}{\partial x} L \qquad (5)$$

since the susceptibility of the sample is the quantity of experimental interest. Unfortunately, it is almost impossible to evaluate $H\ \partial H/\partial x$ independently.

For a given magnet current and suspension fiber, it is customary, therefore, to lump the constants g, L, $H\ \partial H/\partial x$ into a single apparatus constant $K = g/L\ H\ \partial H/\partial x$, so that Eq. (5) can be written in the form

$$\chi_{sg} = \frac{(m_s + m_{f/2})}{m_s}\ K\ d \qquad (6)$$

A special case of eq. (6) is that when the mass of the fiber is negligible with respect to the mass of the sample. In this case

$$\chi_{sg} = K\ d \qquad (6)^*$$

In other words the deflection will be completely independent of the mass of the sample.

From Eq. (6) it is clear that in order to measure the magnetic susceptibility, two quantities have to be determined. These are the apparatus constant K and the mass of the fiber m_f. The mass of the fiber can be calculated fairly accurately from the measurement length and diameter of the fiber, using the known density of fused silica. The apparatus constant K can be evaluated by observing the deflection of a sample of known susceptibility. There are, however, several factors which complicate this evaluation.

(1) The standard sample of known mass and known susceptibility is contained in a tube of known mass but unknown susceptibility. (Although the tube usually consists of fused silica, for which an accurate value for the susceptibility may be found in the literature, commercially available silica seems to show considerable variation in χ_g. Sometimes tubes made of the same silica stock give different susceptibilities depending on the way of heating during attachment of the supporting hook). Since χ_g in Eqs. (6) and (6)* is the mean susceptibility of the combination sample-plus-tube, generally it is not accurately known.

(2) L is not strictly a constant because of the elastic and thermal properties of silica, nor even necessarily the same for F_1 and F_2, since for the latter it refers to the center of mass of the sample-plus-tube combination, which will vary according to the depth of filling of the tube with the sample, while for the former it refers to the center of susceptibility which may or may not be coincident with the center of mass.

Two measurements, however, with a sample of known susceptibility confined to approximately the same position in the same sample tube, lead to an evaluation of the apparatus constant sufficiently accurate for most purposes.

B. Apparatus Calibration

The following procedure is used for calibrating the apparatus:

(1) A sample tube, weighing a few milligrams is prepared from clean, thin walled silica tubing. A fine hook is fused to the tube, and the tube with the hook is boiled in 6M HCl for a few times to get rid of any ferromagnetic impurities. The tube is dried and weighed to ± 5 ugm on an essay balance.

(2) The mass of the hook from which the sample tube is suspended is estimated from its length and diameter and added to the mass determined in (1) above to give the effective mass of the tube, M_o. (Since tube and hook are both made of fused silica they are assumed to have the same susceptibility).

(3) The tube is suspended in the susceptibility apparatus, and its position with reference to the filar micrometer hairline and scale in the telescope is noted and recorded.

(4) The reading of the drum of the precision micrometer located on the head of the susceptibility apparatus is noted and recorded.

(5) The magnet current is successively adjusted to the selected values of 0.5, 1.0, 1.25, 1.75, 2.00 amps.

(6) The image of the sample in the filar micrometer eye pieces is restored to that position noted in (3) by turning the drum of the precision micrometer, and the new reading recorded for the various magnet current settings.

(7) The deflection of the tube, d_o, is taken as the difference of the readings (4) and (6); three readings of this deflection are usually taken and averaged. If, when the magnet current is turned on, the sample undergoes a rotation in the field, the threaded screw which supports the quartz nub to which the suspension fiber is attached is rotated until no rotation of the sample is induced by the magnetic field.

(8) Deflection measurements are made at room temperature and at liquid-nitrogen temperature. The deflection should be independent of temperature within the experimental error of ± 1%. This would indicate that the tube is free of paramagnetic and ferromagnetic impurities,

since the diamagnetic susceptibility of the tube is independent of temperature. If the deflection at liquid nitrogen is much less than that at room temperature, the tube is unloaded and boiled again in 6 M HCI.

(9) A known mass, m_s, of a paramagnetic substance of known susceptibility, χ_{sg}, is added to the tube. This mass which is normally of the order of 100 ugm. is weighed on the sub-microgram balance within ± 0.1 ugm. New deflection measurements d_1, and d_2 are made at two known temperatures--usually room temperature T_1 and liquid nitrogen temperature T_2. Nickelous Ammonium sulphate Ni $(NH_4)_2(SO_4)_2 \cdot 6H_2O$ is used as a reliable standard for susceptibility measurements.[7] Nickelous Ammonium sulphate crystals from Baker and Adamson lot No. 7 were vapor equilibriated with a saturated solution of Ni $(NH_4)_2(SO_4)_2 \cdot 6H_2O$. Its susceptibility is assumed to be given by the relation[8]

$$\chi_g \ (\mathrm{Ni}\ (NH_4)_2(SO_4)_2 \cdot 6H_2O) = \left(\frac{3174}{T+2.5} - 0.3\right) \times 10^{-6} \text{C.g.s.}$$

C. Calculation of Parameters:

Taking the deflection of the empty tube to be d_o, and independent of temperature, its mass (including the hook) to be M_o, its susceptibility to be χ_o, the mass of the calibrating substance to be M_s, its susceptibility at temperature T_1 to be χ_{s1} and at T_2 to be χ_{s2}, and the deflection with the standard in the tube to be d_1 and d_2 at temperatures T_1 and T_2 respectively, the following two equations can be written:

$$(M_{f/2} + M_o + M_s)\ g\ d_1 = (M_o\chi_o + M_s\chi_{s1})\ H \frac{\partial H}{\partial x}\ L \qquad (7)$$

$$(M_{f/2} + M_o + M_s)\ g\ d_2 = (M_o\chi_o + M_s\ \chi_{s2})\ H \frac{\partial H}{\partial x}\ L \qquad (8)$$

Put $(M_{f/2} + M_o + M_s) = M_T$ (i.e total mass) and

$g/H \frac{\partial H}{\partial x} L = K$ as in equation (6)

$$M_T K d_1 - M_o \chi_o = M_s \chi_{s1} \tag{9}$$

$$M_T K d_2 - M_o \chi_o = M_s \chi_{s2} \tag{10}$$

Solving Eqs. (9) and (10) simultaneously

$$K = \frac{\begin{vmatrix} M_s \chi_{s1} & -M_o \\ M_s \chi_{s2} & -M_o \end{vmatrix}}{\begin{vmatrix} M_T d_1 & -M_o \\ M_T d_2 & -M_o \end{vmatrix}} = \frac{M_s}{M_T} \frac{\chi_{s2} - \chi_{s1}}{d_2 - d_1} \tag{11}$$

$$\chi_o = \frac{\begin{vmatrix} M_T d_1 & M_s \chi_{s1} \\ M_T d_2 & M_s \chi_{s2} \end{vmatrix}}{\begin{vmatrix} M_T d_1 & -M_o \\ M_T d_2 & -M_o \end{vmatrix}} = \frac{M_s}{M_o} \frac{\chi_{s2} \, d1/d2 - \chi_{s1}}{1 - d1/d2} \tag{12}$$

So by measuring the deflection of a given sample at two different temperatures and using Eqs. (11) and (12) both K and χ_o can be determined.

A different value of K will be obtained for each different current setting. If a new sample position is chosen, it is necessary to redetermine K for each current at that new position. According to Eq. (6), for the same given sample at two different positions, $K_1 d_1 = K_2 d_2$, where K_1, d_1 are the apparatus constant and deflection at position (1) and K_2, and d_2 those at position (2). So the apparatus constants at various positions can be determined from the apparatus constant at one specified position and the ratio of the deflections at that specified position and other positions. χ_o is determined at different current settings and the average is taken as the susceptibility of the tube.

Once K has been evaluated, the approximate value of M_f may be checked

$$M_{f/2} = M_o \left(\frac{\chi_o}{K d_o} - 1 \right) \tag{13}$$

Calculating the susceptibility of the blank tube from Eq. (12) is susceptible to an error because of the small denominator. A small experimental error in the determination of the ratio d1/d2 will contribute to an appreciable error in χ_o. Therefore the value of χ_o can be checked using Eq. (6) and the determined K Values. For any tube of mass M_o and deflection d_o (independent of temperature)

$$\chi_o = K\, d_o\, (M_o + M_{f/2})\, /M_o$$

For a known weight of sample M_x of unknown susceptibility, run in a tube of mass M_o and susceptibility of χ_o, giving deflection d

$$\chi_x = \frac{(M_o + M_{f/2} + M_x)}{M_x} Kd - \frac{M_o \chi_o}{M_x} \qquad (14)$$

The apparatus used for measurements down to 77^oK is sketched in Fig. 2. Samples are suspended in a quartz tube inside a quartz dewar by a very fine fiber of fused silica of about 44-cm in length.

The tube and dewar assembly, which constitute a single unit, are suspended from a heavy dural ring which is supported by a metal frame attached to the electromagnet.

The dural ring contains an inner, removable brass ring which serves as a support for the fiber attachment. The brass ring is mounted on a micrometer which allows the deflections to be measured by a null method, in which the sample is always restored to the same position in the magnetic field. In this way possible errors resulting from variations in $H\partial H/\partial x$ with sample position are minimized. The suspension fiber can also be rotated to bring an asymmetric sample to a position of zero rotational torque in the magnetic field resulting from its asymmetry. The hole in the ring is closed with a quartz plate. The deflection suffered by the sample under the action of an inhomogeneous magnetic field is observed through the quartz plate by means of a mirror and telescope arrangement. The image of the sample is restored to its initial position with reference to a hair line in

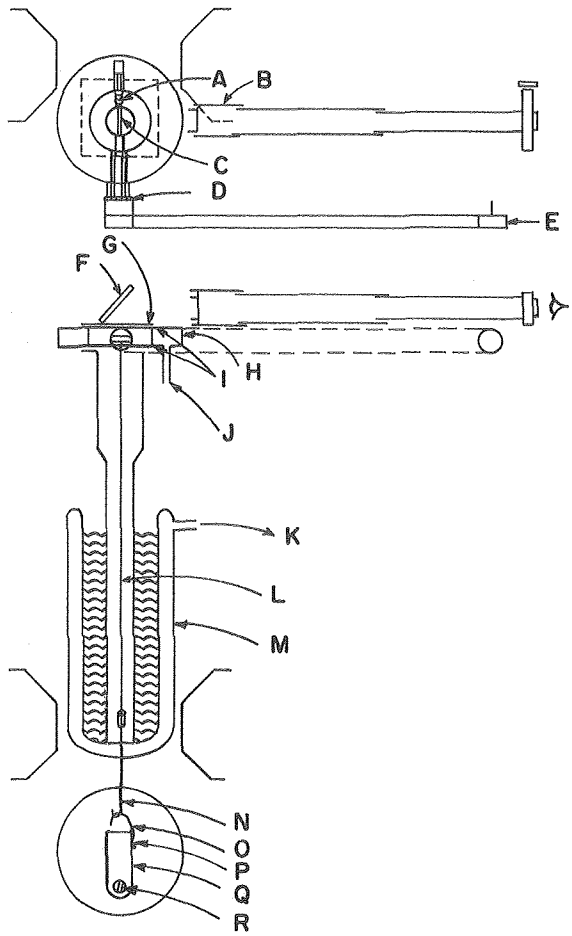

MU-35265

Fig. 2. Magnetic susceptibility apparatus.

Legends of Fig. 2

A. Spring
B. Telescope-filar micrometer system
C. Fiber suspension
D. Micrometer
E. Remote micrometer drive
F. Front-surface mirror
G. Glass plate
H. Aluminum head assembly
I. O-ring seals
J. To vacuum and helium lines
K. To vacuum
L. Quartz fiber
M. Dewar
N. Quartz hook
O. Quartz hook sealed to the tube
P. Araldite epoxy joint
Q. Quartz tube
R. Sample

the filar micrometer by adjusting the micrometer attached to the fiber suspension. The positioning micrometer can be read to an estimated ± 0.5 microns. The magnetic field is produced by an electromagnet with pole faces shaped to give an inhomogeneous magnetic field. All experimental susceptibilities were determined at five different current settings if possible with $H\partial H/\partial x$ varying from 9.5×10^3 to 43.4×10^3 gauss^2/cm. This enabled a correction to be made for any ferromagnetic impurities present in the sample and also made it possible to detect any transitions from paramagnetic to ferro or anti-ferromagnetic in the sample. All measurements were made under 1/3 atmosphere of helium, to assist in the rapid attainment of thermal equilibrium.

The following temperature baths were used:

	^oC	^oK
Ice - H_2O	0	273
Freon 22(monochlorodifluoro methane)	-40.8	232.2
Alcohol - dry ice	-75	198
Freon 14(Carbon tetrafluoride)	-128	145
Liquid nitrogen	-196	77

For temperatures between room temperature and 100°C warm water is passed through a brass U tube which is immersed in the water-filled dewar. The warm water is obtained by passing tap water through a brass coil placed in boiling water. Cold water is allowed to enter from the free end of the coil and exit from the free end of the U tube. The water of the dewar is stirred gently. By adjusting the rate of flow of water, different temperatures can be reached.

In order to make high temperature measurements the sample was suspended in a quartz tube which was surrounded by an oven consisting of a copper block heated by a platinum winding.

The major problem in the measurement of the magnetic susceptibility of microgram samples is the contamination of the sample with trace amounts of ferromagnetic impurities. Care must be taken to handle the tubes and samples only with gold tipped forceps. Even with these precautions several of the samples apparently contained ferromagnetic impurities

since the susceptibility was found to be slightly field dependent. In presence of these impurities the susceptibility of the sample was determined by extrapolating the apparent susceptibility against the reciprocal of the current to $1/i = 0$. This is equivalent to extrapolating to infinite magnetic field where the ferromagnetic impurity is saturated and does not contribute to the measured susceptibility.

III. OPERATION OF MAGNETIC SUSCEPTIBILITY APPARATUS

The principle of the apparatus and the method of calibration have already been described in the preceding section.

What is intended here is a description of the practical aspects of susceptibility measurements.

A. Preparation of Suspension Fibers

Suspension fibers are prepared as follows:

(1) A 3-7 cm length of quartz rod of diameter 0.4 to 0.8 mm is selected and several mm of one end are cemented to a glass slide with glass apiezon wax as shown in Fig. 3 (1)

(2) The attached rod is wiped with Kleenex to remove dust particles.

(3) A hook is formed at the free end by heating with a micro torch as shown in Fig. 3 (2)

(4) The slide is supported by means of a clamp so that the fiber projects 2-3 inches beyond the bench top. Fig. 3 (3)

(5) A platinum weight, made from 1-2 cm of 10-30 mil platinum wire bent in the form of a hook is suspended from the bottom of the fiber.

(6) The rod is heated to softening with a micro torch at a point one cm above the hook, and the torch is held in place until the hook has dropped about 50 cm producing a fiber of 3-20 microns in diameter. Fig. 3 (4)

No amount of description can provide a sure guide to success in this operation. The diameter of the original quartz rod, the mass of the weight, and the size and temperature of the flame all affect the result, which often amounts to breakage or melting of the fine fiber before the pulling is completed. A few practice tries, however, usually give sufficient experience to insure a reasonable probability of success. It was found that a fairly large hot flame seems to give the best results.

(7) Once the fiber has been made, it is necessary to mount it in a manner convenient for subsequent use. A satisfactory method consists of sticking the upper and the lower ends to a flat backing, using a small square of sticking tape.

(8) A flat sheet of dural is wrapped crosswise with scotch tape, such that the distance between outer edges is the correct length of the fiber to be used in the susceptibility apparatus. The taped dural is sprayed with black paint, to render the fine fiber more readily visible.

The painted sheet is placed in back of the fiber and the upper end taped down as shown in Fig. 3 (4). The fiber is cut with scissors above the tape. The lower end is then taped in place and the fiber cut below the tape.

(9) A quartz hook for the lower end of the fiber is prepared from about 6mm of 50-100 micron diameter fiber. A large hook is first formed and then cut to a short v shape of about 3 mm height by scratching with a carborondum (silicon carbide) chip and breaking with a forceps.

(10) The end of the fiber is placed under a binocular microscope, with the backing plate properly supported. One arm of the hook moistened with freshly prepared araldite adhesive and, holding the other arm in forceps, the sticking arm is touched to the mounted fiber just beyond the edge of the cross tape as shown in Fig. 3 (5). Here a short section of the fiber is raised up out of contact with the backing. The epon will hold the hook firmly to the fiber, and normally it is left overnight to form a permanent bond.

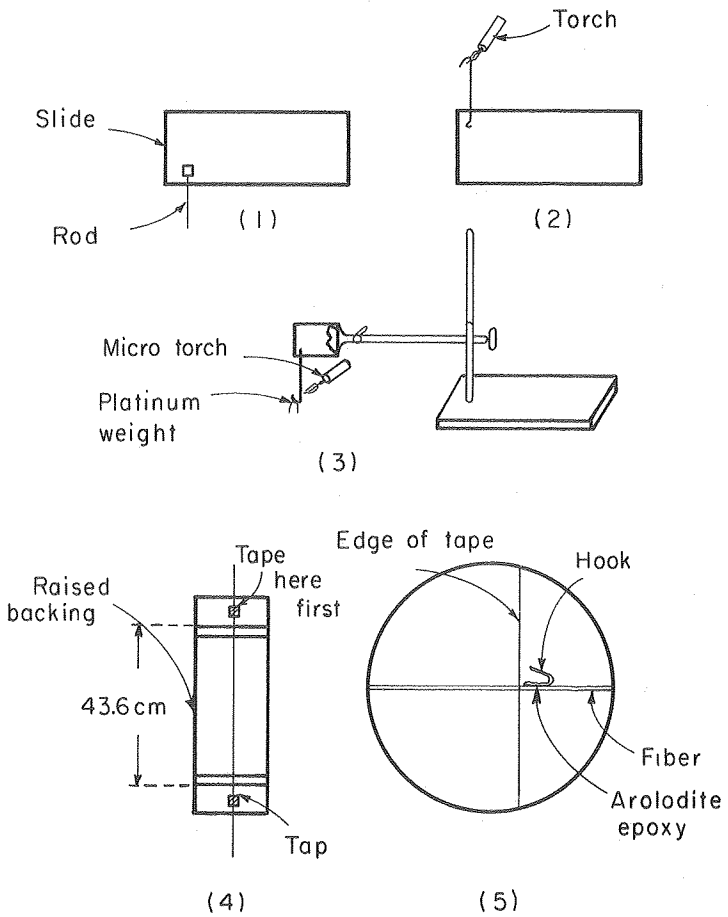

MU-35266

Fig. 3. Preparation of the fiber.

Great care must be exercised in this step in order not to cement either the fiber or the hook to the backing plate. This can be achieved by raising the cemented part of the fiber and the hook slightly above the backing plat. (For high temperature measurements fused junctions are used in place of epoxy seals. This is done as follows: The hook is placed on the edge of a glass plate with the end to be fused projecting over the edge. Using a very fine quartz rod, the end of the fiber is raised up and placed on the projected end of the hook. With a micro torch the fiber is heated gently at first, then strongly with a fairly hot flame to fuse it to the fiber. The flame must not be so strong as to bend the hook. Under the microscope, however, one can see when the fiber is fused and it does not take much time to choose the right flame.)

(11) After the araldite epoxy is set, or the hook is fused to the fiber, the opposite end of the fiber is fastened to the threaded brass supporting nub, at a distance of 43.6 cm from the bottom of the hook. This is done as follows:
A few chips of black apiezon are dropped into the hole at the end of the brass supporting nub. A short length of quartz rod which fits into the hole, and which has been drawn to a fine, coaxial tip is pushed into the hole and the nub is heated until the apiezon melts. A small amount of araldite adhesive is placed on the tip.

The other end of the fine fiber is now cut to the appropriate length, and the cut end is laid on the araldite coated tip of the quartz rod, and left overnight to form a permanent bond. The excess fiber below the hook is cut off, by pressing the edge with a silicone carbide crystal fastened in a glass rod.

Before attempting to move the fiber a quartz tube or other light weight is hooked to the lower end to keep it vertical otherwise room air currents may literally tie it in knots. The brass supporting ring which is screwed to the brass nub is raised so that the fiber is in a vertical position.

The ring is screwed onto the end of the loading rod, and the fiber is withdrawn into the loading tube. Before withdrawing the

fiber it can be cleaned of any dust particles or tiny fine fibers which may have come onto it during preparation. This can be done by carefully passing a fine quartz rod along the fiber for several times.

B. Preparation of Sample Tubes

Sample containers should be light, strong, and of low temperature independent susceptibility. They should have chemical resistance to 4-6 M HCI, and to organic solvents like alcohol and acetone, to permit easy cleaning. Containers made of fused silica or of any of a number of organic polymers satisfy these requirements. Silica tubes have been used throughout the work described here. They are from 0.5-1 mm in diameter and 5-10 mm in length. Larger sizes should be avoided because of the relatively sharp magnetic field gradients.

The tubes are prepared from thin wall silica tubing of appropriate diameter, previously prepared by hard pulling from clean, light wall tubing of about 1 cm diameter. Before pulling the large tubing it should be cleaned with detergent and distilled water, rinsed with alcohol and air dried.

The large tube is rotated in the flame before pulling in order to produce small diameter tubing of circular cross section, since this will minimize the problem of rotation in the magnetic field.

The prepared semicapillary is cut into lengths of about 10 cm by scratching with a silicon carbide crystal, and stored in a closed container. Tubes are prepared from the semicapillary as follows:

(1) A section of the thin wall tubing is grasped near one end with cork-tipped forceps while the other end is held in the right hand.

(2) The tube is heated with a micro torch about one cm from the forceps-held end, which is merely supported while the tube is rotated with the fingers of the right hand.

(3) After a section of the tubing has been heated uniformly to softness a quick push with the forceps and a simultaneous pull with the right hand will draw the heated section to fiber thinness.

(4) The fiber is scratched close to the left hand constriction and broken off. Any hole remaining is sealed by heating the bottom of the tube with the micro torch. In this way the bottom closure will be thin and axially symmetric. Sometimes, however, it is considerably distorted. It can be rounded by closing the open end with apiezon wax and heating the closed end with a micro torch. The increase in pressure inside the tube due to the heating will suffice to expand the bottom into a hemispherical form. The apiezon is then dissolved in CCl_4.

(5) A hook for the tube is prepared from a quartz rod of 60-100 micron in diameter. About 10 cm in length of that fine quartz rod is bent into a hook. The hook is now broken off in such a manner that one arm is a little longer than the other.

(6) The hook is attached to the tube as follows:

For low temperature measurements araldite adhesive is satisfactory. The end of the longer arm of the hook is covered with araldite. Holding the other arm with forceps, the araldite coated end is touched to the tube near the open end. The hook will stick to the tube and it can be adjusted to the required position. It is left overnight where it will form a permanent bond.

For high temperature measurements the hook is fused to the tube. This is done as follows:

The tube is placed on a glass plate in such a manner that about 2 mm from its open end it is projecting over the edge of the plate. About 10 cm of the fine quartz rod is placed on another plate, which will be parallel to the first plate and about one cm apart. The quartz rod is moved until it touches the bottom of the tube about one mm from the open end. The quartz rod is heated, gently at first, then strongly till it fuses to the tube.

The tube is held in cork-tipped forceps, and the quartz rod is bent in a form of a hook at distance of about 0.3-0.5 cm from the open end. The free end of the quartz rod is broken at a distance of 0.2-0.4 cm from the bent place, leaving the tube with the required hook.

After preparing several tubes, they are cleaned by boiling in several changes of 6M HCl. Finally the tubes are boiled in conductivity water and allowed to cool. After drying they are stored in a small screw capped vial. The majority of tubes prepared in this way are free of para or ferromagnetic impurities.

Filling sample containers. A piece of lucite of about 2-3 cm in length and 1-2 cm in width, is prepared with several holes of different sizes. The lucite block is cleaned by washing with concentrated HCl and then water.

The sample container is placed in one of the holes, which will keep it in a vertical position.

For filling with non radioactive samples like nickelous ammonium sulphate and neodymium oxide, a micro spatula made of platinum is used. The transfer usually is not quantitative since some of the powder stays on the top of the opening of the tube. This is removed by shaking the tube and brushing with a small clean brush.

The cleaned tube is weighed on the submicro balance to determine the weight of the material within ±0.1 microgram. After weighing, the tube is placed in a clean hole in the lucite block to be ready for loading in the apparatus.

For radioactive samples the following method is used:
The lucite block is stuck firmly in an ice-cream carton lit using double face tape. The sample tube is placed in a closely-fitting hole in the lucite block. The carton lid is covered and introduced in the glove box. The carton is then opened, and placed under a microscope located on top of the glove box. The microscope is adjusted so that the tube opening is clearly seen. The sample is picked up with gold tipped forceps. Normally the sample will stay on one arm of the forceps, when the jaws are released. The tip of the jaw holding the sample is introduced into the tube, and touched to the tube. The sample will fall into the tube and settle in the bottom. Care must be taken not to touch the tube from the outside at all.

The lid containing the lucite is covered and transfered to the loading box to be ready for loading.

C. Loading the Apparatus

The loading tube is shown in Fig. 4. It consists of an outer lucite tube of about 62 cm in length and about 9 cm in diameter, and an inner concentric tube of about 52 cm in length and 3 cm in diameter. The lucite tubes are sealed together with two lucite plates, one at the top and the other at the bottom. A brass rod of about 56 cm length, which is threaded at the bottom to fit the brass ring of the apparatus, can go in and out the inner tube.

For loading a cold sample the brass rod is lowered until the hook of the fiber reaches a position which can be easily reached. The lucite block which holds the sample tube is brought underneath the hook of the suspension fiber and the sample tube is hooked to the fiber. The lucite block is pulled down slowly, leaving the sample tube hooked to the fiber. The fiber is withdrawn inside the tube and the door of the loading tube is closed.

The loading tube is transferred to the apparatus where it will be placed on a flat lucite plate with an opening in the center. The lucite plate serves to keep the loading tube stable during loading. The fiber is lowered slowly until the brass ring settles in place in the dural ring. The brass rod is unscrewed from the brass ring and pulled into the loading tube. The two screws which hold the brass ring in place are tightened, the lucite plate is removed and the apparatus opening is covered.

For loading an active sample, the same procedure is followed except that the loading is done in a specially designed glove box. The only thing of importance here is that a blank tube or other weight must be hung on the fiber before introducing into the box, to prevent blowing of the fiber and sticking to the box. The normal high velocity air flow in the box is interrupted during loading.

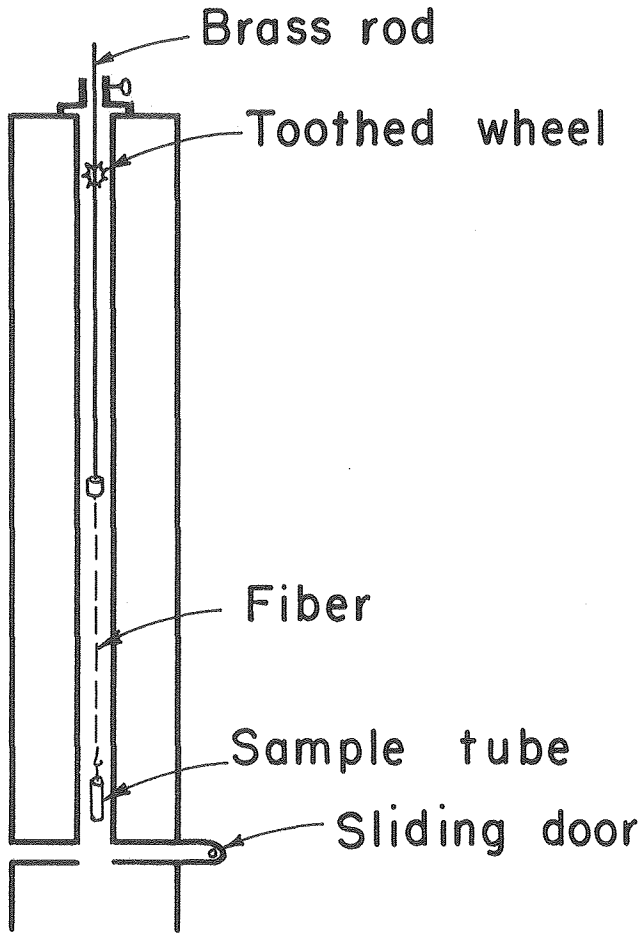

MU-35267

Fig. 4. Loading tube.

D. Observing the Sample and Adjusing Its Position

The mirror is adjusted on the top of the apparatus opening, and the sodium lamp which illuminates the sample from the bottom, is switched on. By looking in the telescope the image of the sample tube can be seen. The telescope is moved until the best focus is achieved. The fiber micrometer is adjusted and the zero point chosen.

While looking in the telescope the current is turned on, and the deflection of the sample is observed. If there is any rotation then the position of the sample is changed by rotating the nub which supports the fiber in a direction opposite to that of the sample rotation.

After adjusting for rotation, the cover of the apparatus opening is placed firmly on the opening and the apparatus is evacuated. The evacuation must proceed slowly in order not to disturb the sample. The apparatus is flushed with helium and evacuated again. This process is repeated twice. After flushing with helium the apparatus is filled with about one third atmosphere of helium. Now everything is ready for taking the measurements.

E. Making Deflection Measurements

The deflection is measured by the null method. The micrometer reading with the current off is taken three times. The current is then turned on and the image of the sample tube is brought to the same position it occupied with the current off. The new reading of the micrometer is taken, and is repeated three times and averaged. The difference between the average reading with the current on and the average reading with the current off is the deflection at this current setting. These measurements are carried out for the current settings (1.0, 1.25, 1.75, 2.0 amps). After all the measurements at all current settings are taken, the whole process is repeated three times, and the deflections are averaged for each current and temperature setting.

F. Unloading the Sample

After all measurements at different temperatures are taken the sample is unloaded. The unloading process is almost the reverse order of the loading. The active samples are stored in the loading box for further measurements.

IV. PREPARATION OF MATERIALS

A. Preparation of Curium Metal

The preparation of pure, well crystallized lanthanide and actinide metals has proved a formidable task. The heat of formation of their compounds is very high, and, consequently, attempts to make the metals by classical techniques have failed. An excellent review of the history of the rare earth metals has been written by Trombe.[9] He points out that the metals are very reactive and that it is even difficult to find materials from which to make crucibles. During the second world war exhaustive studies were made on the preparation of plutonium metal. The methods devised in the Metalurigical Laboratory have been summarized by Fried et al.[10] They centered around the reduction of an actinide fluoride with an alkali or alkaline earth metal. The reductions were carried out in a double crucible system made of a refractory oxide such as beryllia or thoria, and the crucible system was heated in vacuum by resistance heating.

Curium metal (using Cm^{242}) was first prepared on the micro gramme scale by Wallmann, Crane, and Cunningham[11] by reduction of CmF_3 with barium vapour at 1275°C. A double crucible system in a high vacuum system similar to that described by Fried and Davidson[12] was used. The quantities prepared were rather small, ranging from about 0.01 to 4 ug. The metal prepared was silvery in appearance and about as malleable as plutonium prepared under the same conditions. The metal retained its bright appearance in the dry box for some hours but gradually tarnished, and on standing for about 24 hours was rather badly corroded. Under the same conditions, samples of other actinide metals, such as americium or plutonium, have shown less evidence of reaction. The greater reactivity of curium may be attributable to self heating by radioactive decay of the isotope Cm^{242} (equivalent to a power output of 1.2×10^{-4} watts per ug). A sample of Cm^{242} metal, even though it is only partially isolated from its environment may reach high temperatures, which would account for the rapid corrosion rate.

Wallmann and Cunningham indicate that in their work these methods were seldom more than 50 percent successful, because the product often soaks into the refractory oxide crucible.[13] As

a result of their experiments, they suggest using an all-tantalum double crucible system and a wet precipated fluoride. The former leads to more reproducible reduction conditions, and the latter is easier to handle on the microgram scale than fluoride prepared by hydrofluorination. They also found it more convenient to use induction heating.

McWhan, Cunningham, and Wallmann[1,2] described in detail the preparation of americium metal. They used an all-tantalum double crucible system for preparing americium metal from dry americium trifluoride and barium metal.

Cunningham and Wallman[3] prepared curium metal for their crystallographic studies using barium metal as a reductant for curium trifluoride.

Curium metal used for the magnetic measurements is prepared following the same procedure as in the last reference. However, the discussion of the variables which will affect the preparation of good metal will be useful. These variables that will be considered are:

(1) choice of reductant metal,
(2) physical form and treatment of starting materials,
(3) type of crucible system,
(4) reduction temperature and duration of reduction,
(5) method of heating.

1. Reductant Metal

The reaction used to prepared curium metal is the following

$$Cm\,F_3 + 3/x\,M = Cm + 3/x\,M\,F_x$$

From the reaction, it is clear that the choice of the reductant metal is limited by two factors:

(a) The ΔF for the reaction must be thermodynamically favorable.

(b) the vapour pressure of the reductant metal must be sufficiently high to permit vaporization of the excess in a reasonable time without a substantial loss of curium.

Table I lists some reductant metals that satisfy these criteria in the case of americium metal.[2]

Lithium, calcium, barium are possible reductants, and the choice among them is somewhat arbitrary. If lithium is used, the lithium fluoride formed in the reaction vaporizes along with excess lithium more readily than the other cases leaving curium metal only as the product. However, if barium or calcium is used, the barium fluoride or calcium fluoride slag provides a protective coating against surface reactions with the residual gases in the system, and tends to isolate the product from the crucible, making removal of the product easier. Moreover, even a small weight percent of light elements may constitute a high mole percent impurity (0.01 wt.%Li = 0.34 mole %, 0.1 wt.% Ba = 0.17 mole % in curium). As the purity of the metal is of major importance, barium is used preferentially as the reductant metal through all preperations.

2. Physical Form and Treatment of Starting Materials

The first problem of preparing curium metal is that of assuring its freedom from cationic impurities. Because of the scale on which the work had to be done, ordinary reagents were not pure enough. The Cm^{244} used in this study was obtained from neutron irradiated Pu^{239} and was contaminated with rare earths and other decay and fission products.

Curium, as Cm^{+3} was separated from other actinides and rare earths by ion exchange.[14] The curium solution was picked up in the least volume of 0.1 M HCl and transferred to Dowex - 50 column. The column was washed with 0.1 M HCl. This was followed by washing with 2 M HCl until the curium band had moved almost to the bottom of the column. Then the column was washed with 6 M HCl to elute the curium in a minimum volume of eluant. The curium obtained from this process was free of common impurites such as Al, Fe, Ca, and Mg.

Table I. Thermodynamics of AmF_3 reductions.

Reductant	X	ΔF_T (kcal/gram-atom AmF_3)			v. p. (mm)			$T^{\circ}K$, where v. p. of MF_x is 10^{-3} atm.
		1000°K	1250°K	1500 °K	1000°K	1250°K	1500° K	
Li	1	-9	-36	-30	1	30	400	1304
Na	1	-9	+3	+21	180	above b. p.		1322
K	1	-3	+12	+27	650	above b. p.		1142
Ca	2	-48	-45	-39	0.2	10	100	1690
Ba	2	-42	-42	-39	0.1	5	70	1870

T (in °K)	10000	1250	1500
v. p. of Am (in mm)	$3X10^{-6}$	10^{-3}	0.05

The solution obtained from the Hcl column was sorbed on Dowex-50 cation exchange resin followed by desorption with ammonium α-hydroxy isobutyrate at a temperature of 87°C. This process separated curium from the other actinide elements. The solution from the butyrate elution was passed again through a clean-up column to get rid of any impurities that may have been introduced during the last process.

The purity of the resulting stock solution is limited by that of the reagents. It has been found that it is rather troublesome to obtain highly pure acids and bases. Pyrex containers cannot be used, as they introduce significant amounts of calcium, aluminum, and magnesium.[15] Consequently, all work was done in quartz or polyethylene containers which had been leached with concentrated hydrochloric acid. Only water distilled in quartz apparatus was used, and the hydrochloric acid solutions were prepared by distillation in quartz apparatus. The hydrochloric acid was handled in quartz pipettes. The hydrochloric acid prepared in this way was very pure and its spectrographic analysis is shown in Table II. In this way very pure solutions of curium were obtained.

All other reagents used in this work were checked for purity. It should be noted that commercial hydrogen fluoride solutions often contain considerable quantities of aluminum; therefore, hydrofluoric acid solutions were made by vapor equilibration of commercial concentrated HF solutions with quartz-distilled water in polyethylene containers.

It is highly desirable that the fluoride be obtained in the form of compact chunks rather than in the form of powder: first, because powdered material will not yield a single globule of product metal at ordinary reduction temperature; and, second, to maintain ease of loading in the crucible system.

The wet precipitated CmF_3 has the disadvantage that small amounts of oxygen may be incorporated in the final form of the metal. However, the wet CmF_3 is much easier to handle and therefore, reduces the possibility of contamination with ferromagnetic impurities which is of major importance in the magnetic measurements.

Table II. Purity of HCl ugm. per 500 γ HCl

Element	ug. detected	Element	ug. detected
Al	0.01	Mg	< 0.01
Ca	0.02	Na	< 0.01
Cr	< 0.01	Ni	< 0.01
Fe	0.1	Si	< 0.01
K	< 5	Ti	< 0.01

Therefore, curium trifluoride was precipitated from curium hydrochloric acid solution by the addition of excess aqueous hydrofluoric acid to make the final solution approximately 2 M in HF. The precipitation was carried out in a polystyrene centrifuge cone. After centrifuging the precipitate was washed two times with about 40 times its volume of redistilled water (if washed more than two or three times the fluoride peptizes, making quantitative recovery difficult) and two times with similar amounts of absolute ethyl alcohol, centrifuged repeatedly, and the supernatant was drawn off. It was then allowed to air-dry by leaving the cone open to the atmosphere. Upon drying, the trifluoride compacted into a few small pieces of hard translucent material of porcelain - like appearance. This material presumably is hydrated, since air-dried aqueous precipitates of PuF_3 have been shown[16] to contain chemically bound water.

This material was transferred to a platinum container and placed in a desiccator over phosphorous pentoxide. This material was used both for preparing the metal and for measuring the magnetic susceptibility of Cm^{+3} in CmF_3.

3. Type of Crucible System

Ideally, the crucible system should fulfill the following requirements: (a) be unreactive; (b) yield reproducible effusion conditions; (c) keep solid reductant metal from contacting the fluoride; (d) be easy to load; (f) permit easy removal of the product. As mentioned previously, double crucible systems made either from refractory oxides or tantalum have been used in metal preparation. Refractory oxide systems have several disadvantages. They must be fired at 1600 to 1800°C for several hours in order to harden and degas them. The effusion area is not reproducible, and it is difficult to estimate the rate of effusion of the excess reductant and consequently the reduction time. The porosity of the refractory inner crucible is variable. The metal often soaks into the crucible. As a result of these difficulties, tantalum crucibles have been used in the majority of the reduction.

Tantalum has the disadvantage that it is wet by curium metal, and molten curium dissolves appreciable amounts of tantalum. Therefore, at the beginning, the inner crucible has been made in the form of a basket

of 3 mil tantalum wire in order to minimize the tantalum surface exposed. This form of the crucible system is sketched in Fig. 5. The basket holds the fluoride securely. In the event the curium wets the basket, the tantalum can be cut away from the product without appreciable loss. In the measurements made on the metal the presence of tantalum is not of major disadvantage, since its weight can be estimated and its magnetic susceptibility is known.[17]

The inner crucible assembly could be loaded quickly and easily thus cutting to a minimum the exposure of the fluoride and reductant metal to the nitrogen atmosphere of the box. (The dry box, even when flushed with dried nitrogen, is not free of oxygen and water because of diffusion of gases through the gloves.) The size of the hole drilled in the cap of the crucible can be adjusted to fit the desired duration of reduction at the chosen reduction temperature. The rate of effusion from a crucible can be estimated from Knudsen conditions by the equation

$$R \text{ (moles/min./ mm.}^2\text{.)} = 3.5 \times 10^{-2} P_{mm} / M T$$

where
R is the rate of effusion of a gas from the orifice in moles per $mm.^2$ of orifice area, P is the vapor pressure of the curium or barium, M is the molecular weight, T is the absolute temperature. As the system does not match ideal conditions for Knudsen effusion, the actual effusion will be slower than the above estimate. An effusion hole of 1/3 - 1/2 mm is convenient for most reductions.

As mentioned earlier molten curium dissolves an appreciable amount of Ta[3]. Therefore the inner crucible was modified so that the piece of trifluoride was inserted between two parallel tungsten wires held in the tantalum frame, which was then inserted into the crucible. The disadvantage of this technique is the difficulty of inserting the fluoride piece between the two wires and keeping it firmly between them. However, no tungsten was detected by spectrographic emission analysis of samples of curium made by this method

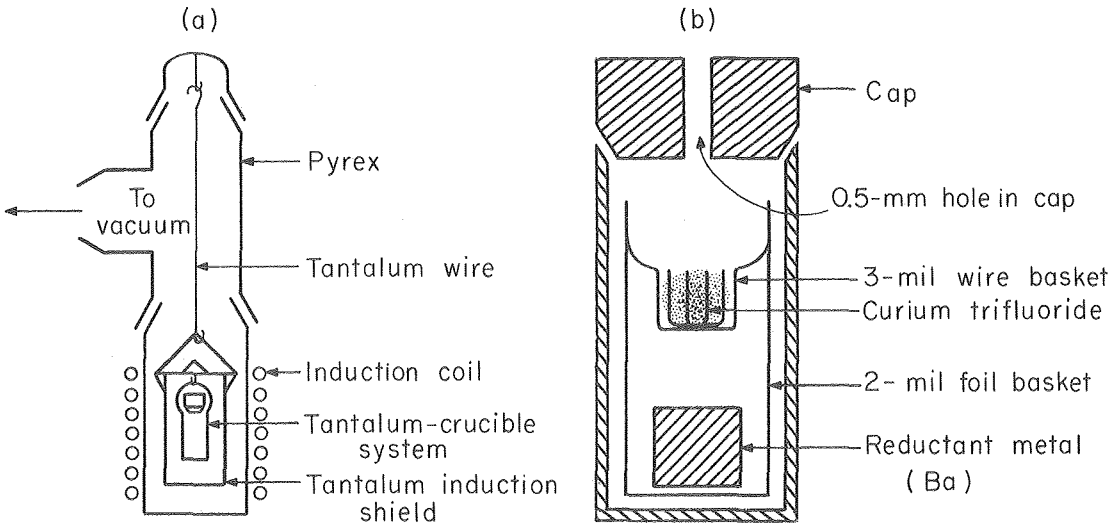

MU-35268

Fig. 5. Apparatus for the reduction of CmF_3 with Ba.
a. Microscale metal-production apparatus.
b. Crucible.

and used for melting point determinations. (analysis and purity of materials are given in Table IV). In addition it is easy to get the metal free or with very small length of tungsten wire.

In later preparations a tungsten spiral was used. The spiral was hooked to the cap of the crucible and the trifluoride piece held firmly in the spiral loops.

4. Reduction Temperature and Duration of Reduction

The reduction temperature is critical. If it is too low, the resulting metal is impure; if it is too high, the metal vaporizes. Reductions carried out far below the melting point of curium (1340°C) contained about 2 mole percent of barium.

The reduction time is dependent on the temperature, size of the crucible orifice, and amount and nature of excess reductant. A significant amount of time is needed for the crucible system to reach the reduction temperature. This can be reduced by initially setting the heater to a kilovolt reading corresponding to a much higher temperature and then cutting back to the desired temperature. In a typical reduction of curium trifluoride, metal of good appearance was obtained in high yield by maintaining a reduction temperature of from 1315 to 1375°C for two minutes. Additional heating for three minutes at 1235°C served to remove excess barium as well as barium fluoride slag. No detectable loss of curium from the crucible system was observed under these conditions. The curium prepared in this way exhibited a silvery appearance and Ba was not detected in most of the samples.

5. Method of Heating

Three methods of heating can be used with varying degrees of success: (a) electron bombardment; (b) resistance heating; (c) induction heating. The choice among them is mainly one of convenience and reproducibility. Electron bombardment is the most efficient, but the measurement of the temperature with an optical pyrometer is uncertain because of the reflection from the filament and the emissivety correction

that has to be made. Far more important is the difficulty of controlling the temperature because of the arcing that occurs when the excess barium effuses from the crucible.

Resistance heating is inefficient, but it provides good temperature control from the reduction temperature to room temperature. As with electron bombardment, the effusion of excess barium can be followed by its green glow. This method has two disadvantages. First, the coil is fragile, and second, the tantalum crucible has to be insulated from the heater.

The induction heater provides accurate temperature control, permits accurate temperature measurements and is easy to use. In a typical experiment, the blank crucible system is assembled and heated to 1000°C to vaporize the copper resulting from spot-welding the tantalum assembly. This step is necessary since otherwise the copper condenses on the walls of the vacuum system during temperature calibration and would lead to an error in the measurement of the temperature if not removed beforehand. For temperature calibration a clean pyrex bulb is put on the line and the temperature of the crucible system, observed under black-body conditions through a hole in the induction shield with an optical pyrometer, is measured and plotted against various Kilovolt settings on the power supply. After cooling, the crucible system is loaded with the fluoride and barium, and then reduction is carried out as described above.

Some of the experimental results showing the characteristics of the samples used in the magnetic measurements described in the following sections are shown in Table III.

Purity of curium metal. Samples of curium were analyzed by spectrographic emission analysis, using copper spark excitation. The spectrographic results for three samples of the metal are shown in Table IV. All quantities are in micrograms. The blanks have been corrected to a volume equivalent to the sample volume. The impurities detected are listed in the top of the table, and limits of detection are listed in the bottom of the table.

Analysis of one sample of metal for oxygen, using ^{3}He activation[18] showed the presence of ≅ 4000 p.p.m.

Table III. Curium Metal Preparations Used in Magnetic Measurements.

No	Reductant	T°C	Time Min.	Cooling	Inner Cruc.	X-Ray	Comments
1	Ba	1040	13	in vac.	Ta basket	good lines dhcp	The first 3 minutes went normally; then the inducution heater would operate for 10 seconds and cut for 10 sec. Metal resulted which had not wet the Ta wires.
2	Ba	1315 1235	2 3	" " "	Parallel W wires	No lines	Product looked very good. The metal wet the wires; used for melting point determination then magnetic susceptibility.
3	Ba	1300 1275 1200 1050	1 5 5 10	" " "	" " "	No lines	The product was metallic looking, had not wet W wires and was easily broken free.
4	Ba	1345 1315 1260 1200 1080	1 1 1 7 1/2	" " "	" " "	No lines	The product looked dark and poor. Surface not smooth. Proved to be malleable.

Table III. Continued

No.	Reductant	T°C	Time Min.	Cooling	Inner Cruc.	X-Ray	Comments
5	Ba	1345 1315 1255 1200 1080	1 1 1 6 1/2 1/2	in vac	Parallel W wires	good lines	Product looked extremely shiny. Surface smooth but not rounded edges i:e had not melted.
6	Ba	1080 1340 1370 1200	1 1/4 1/4 1/2 3	" " "	" " "		The product looked as it had wet the W wires but was not smooth round ball. It seemed brittle when squeezed.
7	Ba	1075 1175 1375 1225	1 1/4 1 1/2 1	" " "	" " "	Some lines dhcp	Product looked good. It had not wet the wires.

Table IV. Purity of Curium Metal.

Sample		Cm	Al	Ba	Ca	Mg	Total Mole%Cm
1.	Sample	18.4	0.01	---	0.05	0.02	
	Blank	---	0.01	0.2	0.03	0.02	
	Mole%	---	---	1.81	0.65	---	97.54
2.	Sample	57.8	<0.05	< 1	0.02	0.01	
	Blank	---	<0.01	< 1	0.01	0.01	
	Mole%	---	---	--	0.1	0.17	99.73
3.	Sample	125	<0.01	<0.01	0.02	0.01	
	Blank	---	<0.01	---	0.02	0.02	
	Mole%	---	---	---	---	---	100

Limits of detection by Cu spark method

Ag	<0.01	Eu	<0.01	<Lu	<0.05
As	<0.05	Fe	<0.01	<Mn	<0.01
Au	<0.5	Ga	<0.1	<Tl	<0.1
Be	<0.01	Gd	<0.05	Tm	<0.05
Bi	<0.05	Ge	<0.05	U	<0.1
Cd	<0.5	Hf	<0.1	V	<0.05
Ce	<0.1	Ho	<0.05	W	<0.1
Cm	<1	In	<0.05	Yb	<0.01
Co	<0.05	Ir	<0.05	Y	<0.01
Cr	<0.01	K	<1	Zn	<0.1
Dy	<0.05	La	<0.01	Zr	<0.01
Er	<0.05	Li	<1		

Mass analysis showed the isotopic composition of curium used in this work to be: Cm^{244} 96.59%; Cm^{245}, 1.59%; Cm^{246}, 1.82%.

B. Preparation of Curium Trifluoride

The fluoride used for the magnetic susceptibility measurements was a portion of the same material used for the metal preparation. The procedure for the fluoride preparation was described in Sec. A.

C. Preparation of Curium Oxychloride

The curium solution which was used for these preparations had been purified as usual.[14] The solution was stored for a long time before use and therefore had a relatively high percentage of plutonium, resulting from the decay $Cm^{244} \xrightarrow{\alpha} Pu^{240}$. It was purified from plutonium by anion exchange. Two to three drops of concentrated nitric acid were added to the curium solution in 6 M HCl so that the final hydrogen ion concentration is around 7 - 8 molar. The solution was heated for 20 - 30 minutes to insure the presence of plutonium in Pu^{+4}. The solution which now containes plutonium as Pu^{+4} complex was transferred to the top of anion exchange column (Ag 1x8, 200-400 mesh size). The column was washed with 6 M HCl where curium was washed and collected in a quartz cone while plutonium was held by the column. Plutonium can be recovered by eluting the column with 0.1 M HCl.

The solution of curium obtained is evaporated to dryness, picked up in 0.1 M HCl and run on a clean-up column to get rid of any impurities introduced by using concentrated nitric acid.

Mass analysis of the curium solution showed less than 0.1% of plutonium. Spectrographic analysis of the solution is shown in Table V (limits of detection are those given in Table IV).

This curium solution was used to prepare curium oxychloride. First curium hydroxide was precipitated by passing ammonia gas through the solution until complete precipitation was achieved. The supernatant was drawn off and the precipitate was washed twice with conductivity

Table V. Purity of curium solution

ugm. of impurity per 50 ugm of curium.

Al	< 0.01	Mn	< 0.01
Am	0.1	Ni	< 0.05
Ca	< 0.01	Pb	< 0.1
Cr	< 0.01	Pu	< 1
Eu	< 0.01	Si	< 0.01
Fe	< 0.01	Ti	< 0.01
Gd	< 0.05	Yb	< 0.01
La	< 0.01	Y	< 0.01
Mg	< 0.01	Zr	< 0.01

water and centrifuged repeatedly. The water appearing on the surface of the precipitate resulting from centrifuging was drawn off. The precipitate was then centrifuged for six hours during which it dried completely and broke into small hard chunks.

The hydroxide pieces were put in a capillary drawn at the end of quartz ground joint. The joint was connected to the apparatus shown in Fig. 6. Fixed concentrations of $HCl_{(g)}$ and $H_2O_{(g)}$ (given at the end of Table VI) carried by a stream of nitrogen from 28% HCl solution were passed over the sample which was heated to 550°C ±5°C. The composition of the HCl - H_2O mixture was suggested by the data of C. W. Koch[19], who measured the equilibrium constants of transformation of americium trichloride to americium oxychloride. The values of the equilibrium constants at different temperatures are shown in Table VI. From the table it appears that the composition of HCl - H_2O mixture at a given temperature is critical. If the value of P^2_{HCl}/PH_2O exceeded the value of the equilibrium constant the reaction will go to the trichloride rather than the oxychloride. The stream of gases was passed over the sample for two hours. Nitrogen was substituted for HCl-H_2O mixture while the sample was still hot. This helped in removing the HCl-H_2O mixture before cooling the sample (otherwise trichloride will be formed at the lower temperature). The temperature was then lowered slowly while nitrogen was still passing through the apparatus. After the sample reached room temperature the ground joint was taken away, the capillary cracked off and the sample stored in a disiccator over magnesium perchlorate.

The curium oxychloride was identified by its x-ray diffraction pattern. No lines were obtained from the sample after about six days from its preparation, probably because of radiation damage of the amorphous material. A few micrograms were sealed in a quartz capillary, heated to about 600°C for annealing and then cooled. The x-ray diffraction pattern was taken on the same day of annealing. A few lines were obtained, comparable to those of AmOCl. No trichloride lines were observed.

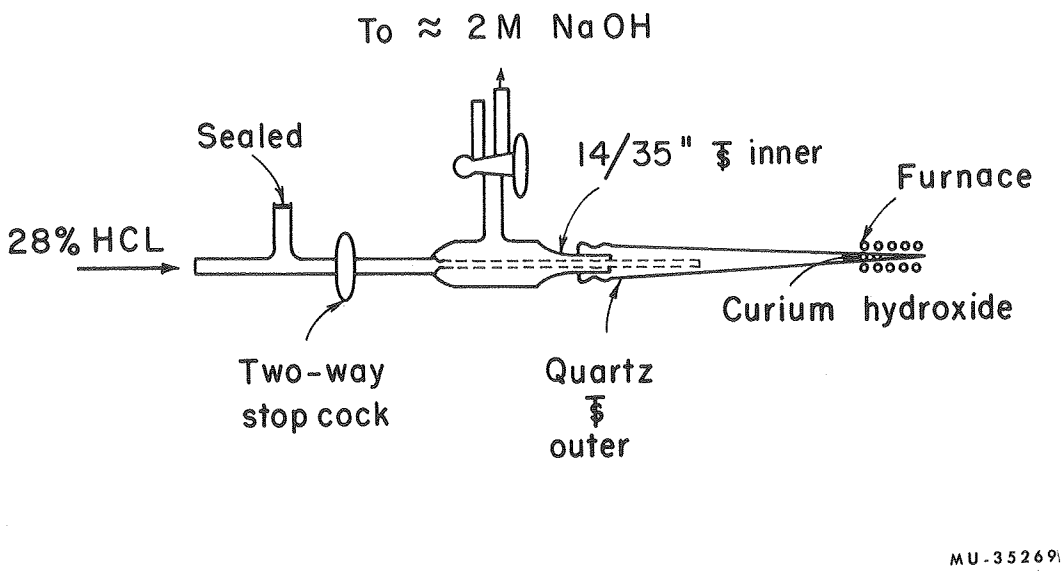

Fig. 6. Apparatus for preparing CmOCl.

Table VI. Equilibrium Constants for the Reaction

$$AmCl_{3(g)} + H_2O_{(g)} = AmOCl_{(s)} + 2HCl_{(g)}$$

°K T	v.p. HCl (mm)	v.p. H_2O (mm)	Kmax / Kmin	ΔFexpt Kcal	ΔFcalc Kcal	Dev. Kcal
880	344 304	2.85 3.34	54.6 50.9	-6.93	-6.96	-0.03
841	323 306	4.12 4.07	33.3 30.3	-5.78	-5.77	+0.01
807	198 179	2.43 2.40	21.2 17.6	-4.76	-4.73	+0.03
789	225 212	4.91 4.46	13.6 13.3	-4.07	-4.18	-0.11
780	178 169	3.31 3.15	12.6 11.9	-3.89	-3.90	-0.01
739	153.6 139.8	4.89 4.76	6.27 5.40	-2.59	-2.66	-0.07
700	94.9 88.1	4.04 3.67	2.93 2.78	-1.46	-1.43	+0.03
682	73.3 67.4	3.43 3.24	2.07 1.85	-0.91	-0.87	+0.04
			Average Deviation			±0.04

Partial Vapour Pressure of HCl at 25°C[20]

%HCl	v.p.H_2O(mm)	v.p. HCl(mm)
28	7.05	8.75
30	15.10	7.52

D. Preparation of Curium Trifluoride in Lanthanum Trifluoride Matrix

Lanthanum oxide (code-529 lot No. 1371) was used as starting material. Ten milligrams of lanthanum oxide were dissolved in quartz distilled hydrochloric acid. About 500 micrograms of curium in 6 M HCl were added and the solution stirred thoroughly. This solution was added to an excess of aqueous hydrofluoric acid to make the final solution approximately 2 M in HF. The supernatant was drawn off, the precipitate was centrifuged for three hours. The mixture dried completely and broke into small hard chunks. The mixture was then heated under vacuum at a temperature of 200°C for dehydration.

A sample of lanthanum trifluoride was prepared under the same conditions. The magnetic susceptibility of this lanthanum trifluoride was measured and the value obtained was used for correcting for the diamagnetism of lanthamum trifluoride in the mixture.

The purity of the materials used in preparing the mixture was checked by spectrographic analysis. The spectrographic analysis results for the curium solutions used and for the quartz distilled hydrochloric acid have already been given in Tables II and V, respectively. The analysis results of the La_2O_3 samples are shown in Table VII.

A small sample of the mixture was dissolved and assayed to determine the mole percentage of curium trifluoride. The results showed 5.6% (mole %) of curium trifluoride in the mixture.

Table VII. Purity of La_2O_3-ugm per ≅500 ugm of La

Element	ug detected	Element	ug detected
Al	< 0.01	Mo	< 0.05
Bi	< 0.05	Nd	< 0.1
Ca	0.02	Ni	< 0.01
Cd	< 0.5	Pr	< 0.1
Co	< 0.05	Sc	< 0.01
Cr	< 0.01	Si	< 0.01
Er	< 0.05	Sm	< 0.05
Eu	< 0.01	Ta	< 0.1
Fe	< 0.01	U	< 0.1
Gd	< 0.05	V	< 0.01
Mg	< 0.01	Yb	< 0.01
Mn	< 0.01	Y	< 0.01

V. RESULTS

A. Curium Metal

The magnetic susceptibility of five samples of curium metal have been investigated, and the results are listed in the following tables. The purity of the samples and the experimental conditions of preparation have already been given in Tables III and IV of Sec. IV. The sample numbers refer to the preparations listed in Table III. Sample 2 showed field dependence which is attributed to contamination with some ferromagnetic impurities due to much handling of the sample. Therefore, the measured susceptibility was corrected for ferromagnetic impurities by plotting the measured susceptibility vs. 1/i and extrapolation to $1/i \doteq 0$ to get the correct value as shown in Fig. 7. The relation between the magnetic field and the current is estimated to be $dh/di \cong 5000 \pm 2000$ gauss/amp.

Sample I was sealed in a quartz capillary and the susceptibility of quartz was assumed to be equal -0.5×10^{-6} c.g.s The apparatus constant used in calculation was estimated from the known susceptibility of quartz and the measured deflection of the quartz tube. In the case of the other four samples both the apparatus constant and the susceptibility of quartz were determined experimentally by calibrating the apparatus with nickelous ammonium sulphate. The error in the apparatus constants varied from 3.0 to 2.2% depending on the current setting. The absolute error in the susceptibility of the standard materials used in the standardization was assumed to be 2%, and this assumption accounts for most of the error in the apparatus constants.

Tables VIII - XII give the gram susceptibility of different samples of curium metal at different tamperatures. Table XI gives the susceptibility of sample 2 at different fields together with the corrected susceptibility which is given in the last column of the table (χ_∞). The deflection in sample five was very small especially at low temperature so that the experimental error was quite large.

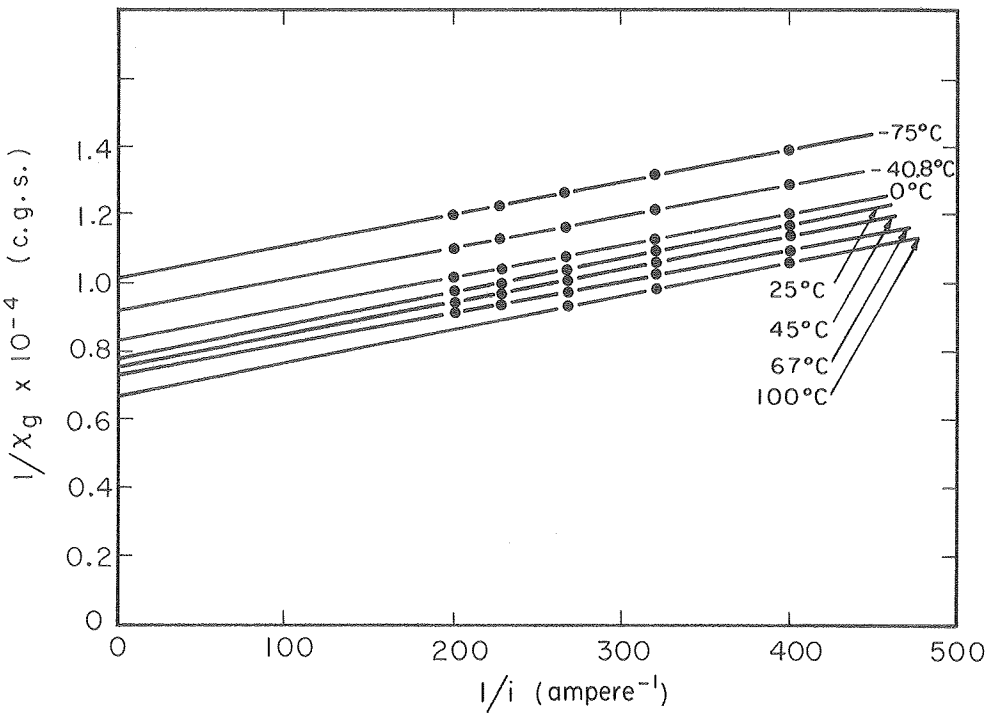

MU-35270

Fig. 7. Correction for ferromagnetic impurities.

Table VIII. Susceptibility of Curium Metal (Sample 1)

$T^{o}C$	$\chi \times 10^{6}$	$1/\chi \times 10^{-4}$
- 196	15.93 ± 0.3	0.627
- 75	10.12 ± 0.2	0.988
- 40.8	9.21 ± 0.2	1.085
0	8.32 ± 0.2	1.202
25	8.08 ± 0.15	1.237
44	7.95 ± 0.15	1.258

$\Delta = 238^{o}$

$\mu_{eff} = 9.2 \pm 0.4$ B.m.

Table IX. Susceptibility of curium metal (sample 2).

T°C	$\chi \times 10^6$						
	1.0 amp	1.25 amp	1.5 amp	1.75 amp	2.0 amp	χ_∞	$1/\chi_\infty \times 10^{-4}$
- 196	249.43±4.1	241.88±4.1	234.54±4	230.95±4	233.29±4	212.00±3	0.471
- 75	139.41±1.5	132.55±1.5	126.94±1.5	123.21±1.1	120. 3±1.0	102.00±1.5	0.980
- 40.8	129.58±1.3	122.1 ±1.3	116.48±1.1	113.16±1.3	110.25±1.2	92.0 ±1.5	1.087
0	120.57±1.3	113.45±1.3	109.06±1.0	104.35±1.0	101.46±1.0	83.5 ±1.5	1.198
25	117.33±1.4	109.9 ±1.3	103.89±1.0	101.07±1.0	97.95±1.0	78.0 ±1.5	1.282
45	114.09±1.1	106.22±1.3	101.42±1.2	97.55±1.0	94.77±0.9	75.5 ±1.5	1.324
67	109.63±1.1	103.23±1.3	98.23±1.3	94.14±1.0	91.84±0.9	73.0 ±1.5	1.370
100	105.95±1.0	98.28±1.8	94.17±1.1	-----	-----	67.0 ±1.5	1.492

$\Delta = 135$ $\mu_{eff} = 8.15 \pm 0.15$

Table X. Susceptibility of curium metal (sample 4)

$T^{o}C$	$\chi \times 10^{6}$	$1/\chi \times 10^{-4}$
-196	126.02 ± 2.5	0.794
- 75	74.55 ± 1.4	1.341
- 40.8	68.40 ± 0.7	1.462
0	62.41 ± 1.2	1.602
25	59.53 ± 0.8	1.680
52	57.03 ± 0.9	1.754
69	55.42 ± 0.7	1.804
100	52.44 ± 0.9	1.907

$\Delta = 224^{o}$

$\mu_{eff} = 7.85 \pm 0.1$

Table XI. Susceptibility of curium metal (sample 5)

$T^{o}C$	$\chi \times 10^{6}$	$1/\chi \times 10^{-4}$
-196	88.43 ± 1.0	1.13
-128	65.79 ± 1.0	1.52
- 75	58.37 ± 1.0	1.713
- 40.8	55.12 ± 1.0	1.814
0	51.18 ± 1.0	1.954
25	50.29 ± 1.0	1.988
50	48.03 ± 1.0	2.082
100	44.84 ± 1.0	2.230
32	48.69 ± 1.0	2.054
52	47.65 ± 1.0	2.099
75	46.34 ± 1.0	2.158
150	42.14 ± 1.0	2.373
253	37.23 ± 1.0	2.686

$\Delta = 348^{o}$

$\mu_{eff} = 7.96 \pm 0.1$

Table XII. Susceptibility of curium metal (sample 7)

$T^{o}C$	$\chi \times 10^{6}$	$1/\chi \; 10^{-4}$
- 196	217.32 ± 4.0	0.460
- 128	86.28 ± 1.5	1.159
- 75	70.52 ± 1.5	1.418
- 40.8	62.81 ± 1.0	1.592
0	56.94 ± 1.0	1.756
25	54.97 ± 1.0	1.819
72	45.60 ± 1.5	1.965
153	42.60 ± 2.0	2.193
202	42.62 ± 1.4	2.346
278	39.44 ± 3.0	2.535

$\Delta = 286^{o}$

$\mu_{eff} = 8.01 \pm 0.1$

The plots of the inverse of the gram susceptibility of different samples vs. the absolute temperature are shown in Figs. 8 - 12. Fig. 7 shows the plot of the gram susceptibility of sample 2 vs. 1/i. This is the only sample which showed field dependence and the only sample for which such a correction was applied.

From the plots it is clear that the metal follows Curie-Weiss law in the temperature range from 300°C to -128°C. This law can be represented in the form

$$\chi_M = C/(T + \Delta)$$

where χ_M is the molar susceptibility, T the absolute temperature, Δ is the molecular field constant or Weiss constant, and C is a constant. The molecular field constant was calculated for the different samples from the plot of $1/\chi$ vs T using the formula

$$\Delta = \frac{\chi^{-1}}{S} - T$$

where S is the slope of the best straight line passing through the points.

The Δ values found for different samples range from 135-348°. The value for each sample is given at the end of the corresponding table. This big change in the Δ values can be attributed to two factors: First, the sensitivity of that value to the slight change in the experimental points on the line; however, this can attribute only to a small factor of the change (± 10°). Second, the possibility of the presence of stacking faults in the lattice of the metal. This change in the Δ value is a real one since there is no actual change of this value for the same sample taken at different times, while the difference is quite large from one preparation to the other.

The effective moments (in Bohr magneton) were calculated for the different samples from the measured susceptibility and the calculated Δ value using the relation[21]

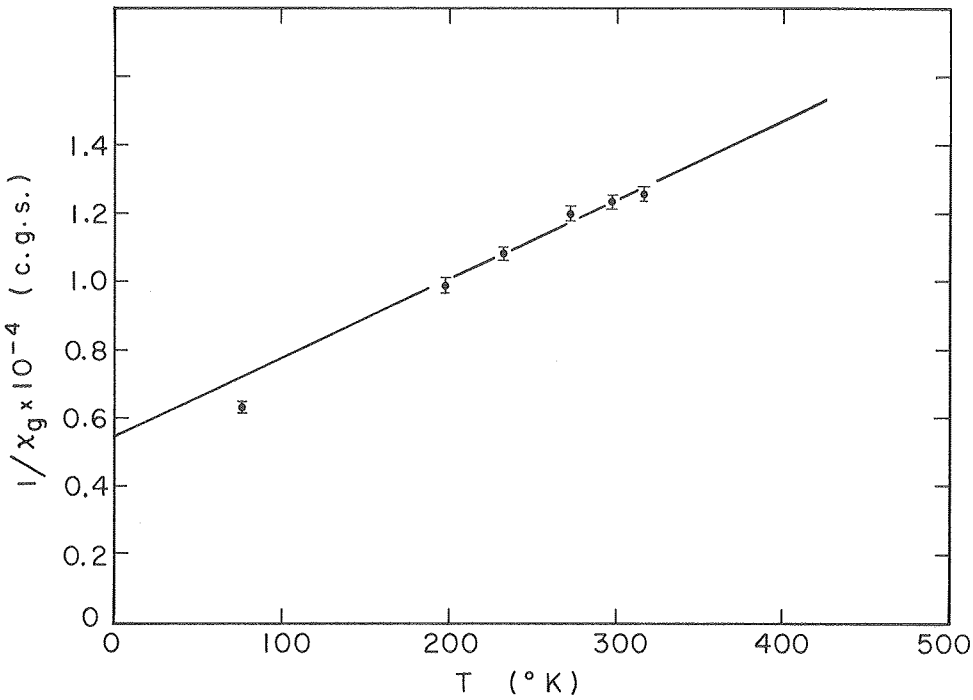

MU-35271

Fig. 8. $1/\chi_g$ vs T(^{o}K) for curium metal. (Sample 1)

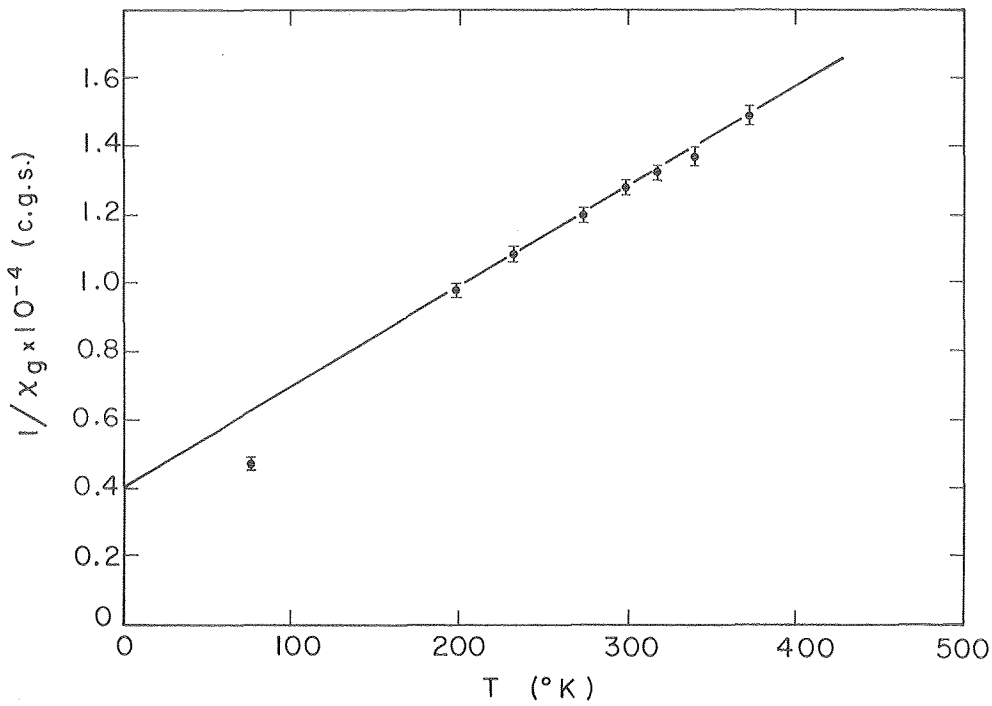

MU-35272

Fig. 9. $1/\chi_g$ vs T(^{o}K) for curium metal. (Sample 2)

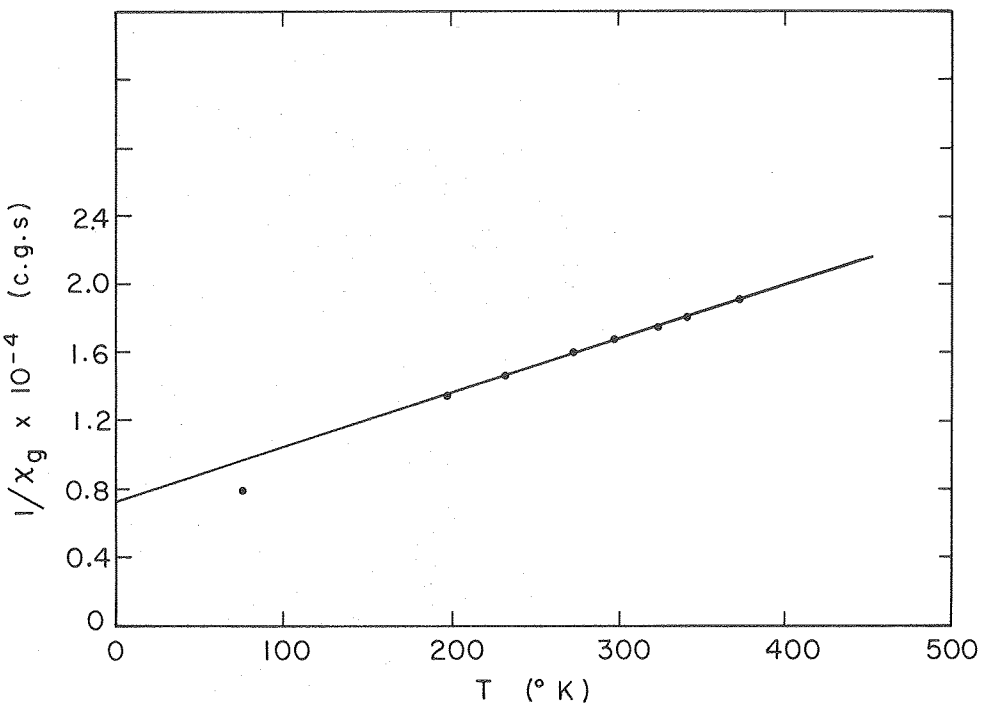

MU-35273

Fig. 10. $1/\chi_g$ vs T(^{o}K) for curium metal. (Sample 4)

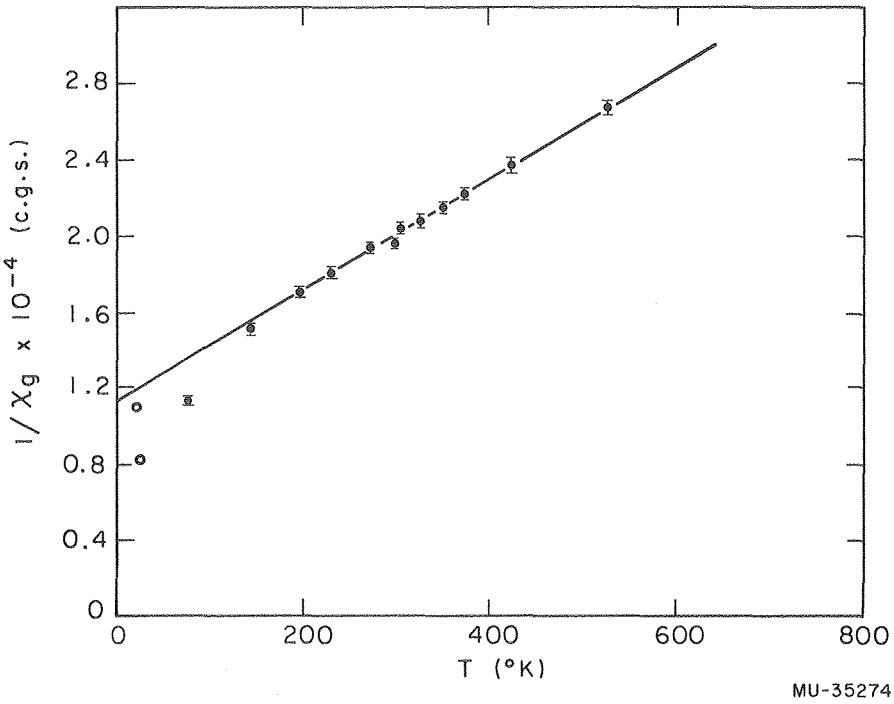

Fig. 11. $1/\chi_g$ vs T(°K) for curium metal. (Sample 5)

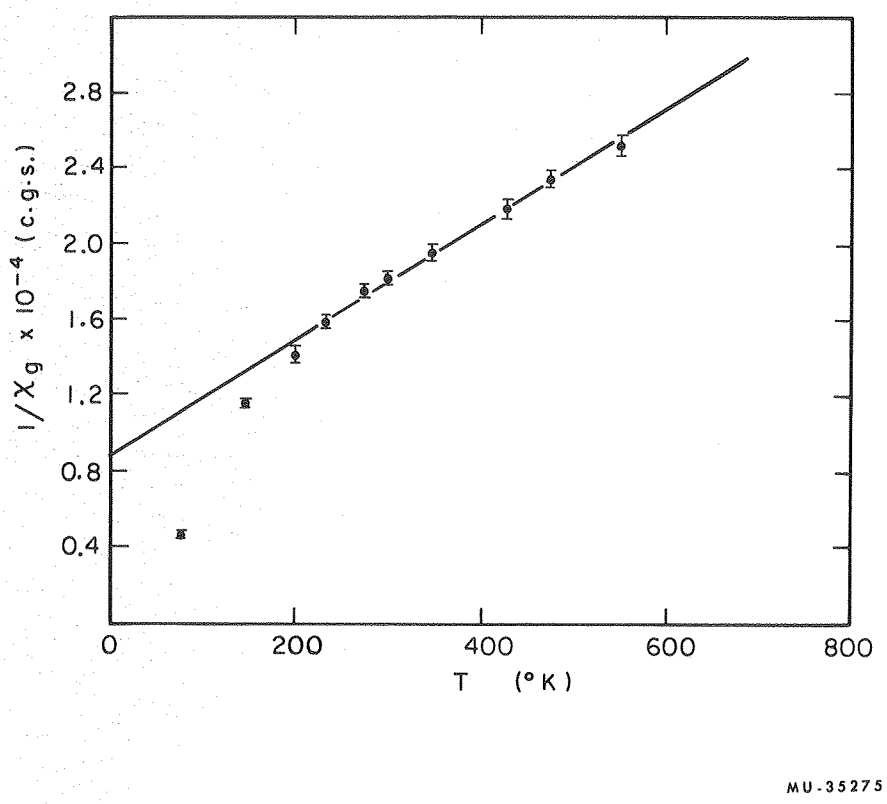

Fig. 12. $1/\chi_g$ vs T(^{o}K) for curium metal. (Sample 7)

$$u_{eff} = \sqrt{\frac{3\ k\ \chi_M\ (T + \Delta)}{N\ \beta^2}}$$

$$= 2.84 \sqrt{\chi_M\ (T + \Delta)}$$

where k is Boltzmann constant, and T the absolute temperature, N Avogadros number, and β the Bohr magneton, the magnitude os which is given by

$$\beta = e\ h\ /\ 4\ \pi\ m\ c = 0.917 \times 10^{-20}\ \text{erg/gauss}.$$

The values obtained from different samples give $u_{eff} = 7.99 \pm 0.1$ for curium metal. The values of the effective moment agreed fairly well from one sample to the other. The effective moment of each sample is given at the end of the corresponding table. The first sample gave a relatively high effective moment of 9.2. The susceptibility of this sample was calculated using the estimated apparatus constant which is a little higher than the determined one.

The effective moment found for the metal agrees very well with the theoretical value of 7.94 calculated for the configuration of $5f^7$ using Russell - Saunders coupling. This value agrees also with the recently determined value of gadolinium metal of 8.07 ± 0.05 with Δ value of -310°.[22]

These results indicate that curium metal consists of tripositive ions and that the Russell - Saunders coupling is still predominatly effective in this range. However, due to the large Δ values found and used in the calculation of the effective moment, no final word about the exact coupling obeyed in the case of the metal can be said.

It is clear from all the graphs that the metal deviates from Curie - Weiss law at liquid nitrogen temperature. This deviation is a real one because it is consistent in all the samples measured in spite of difference in preparation. The deviation is far beyond any experimental error possible. This behavior indicated the possibility of magnetic transition at that temperature. Therefore, magnetic measurements at lower temperatures seemed very useful.

An attempt to measure sample no. 4 at liquid hydrogen temperature (20° K) was carried out. The dewar was shielded by a plastic shield which has a tygon tubing going to the exhaust line. Liquid hydrogen was introduced to the dewar and the reading was taken after one minute from introducing the hydrogen. This point is shown marked with an open circle in Fig. 11. Five minutes later the reading was taken again and the deflection was almost equal to that at liquid nitrogen temperature. When liquid hydrogen was introduced again into the dewar the plastic shield cracked and the experiment was interrupted. Another attempt to keep liquid hydrogen in the dewar failed.

Therefore, the decision to build a new dewar for low temperature measurements was taken. Building of a new dewar led to building of a new apparatus for low temperature measurements. The description of this new apparatus and some preliminary measurements will be given in the following few pages.

Low Temperature Measurements

a. The apparatus. The principle of the low temperature apparatus is the same as the one described in the first section. There are some changes in the assembling of the apparatus. The picture of the apparatus is shown in Fig. 13. The main changes in this apparatus will be described below.

(1) The magnet system. The magnet used here is Varian four-inch electromagnet, Models V 4004, V 2300 A, V 2301 A. It consists of Model V 4004 electromagnet with an air gap which can be adjusted to any value from zero inches to four inches, Model V 2300 A power supply which provides infiltered d.c power for deriving the magnet, and Model V 2301 A current regulator to provide a stable current during the measurements. The current here can be adjusted much better than in the old apparatus.

(2) The dewar. Up to liquid nitrogen temperature it was possible to use a simple two wall dewar with a quartz window at the bottom for passing the light. Below liquid nitrogen temperature it

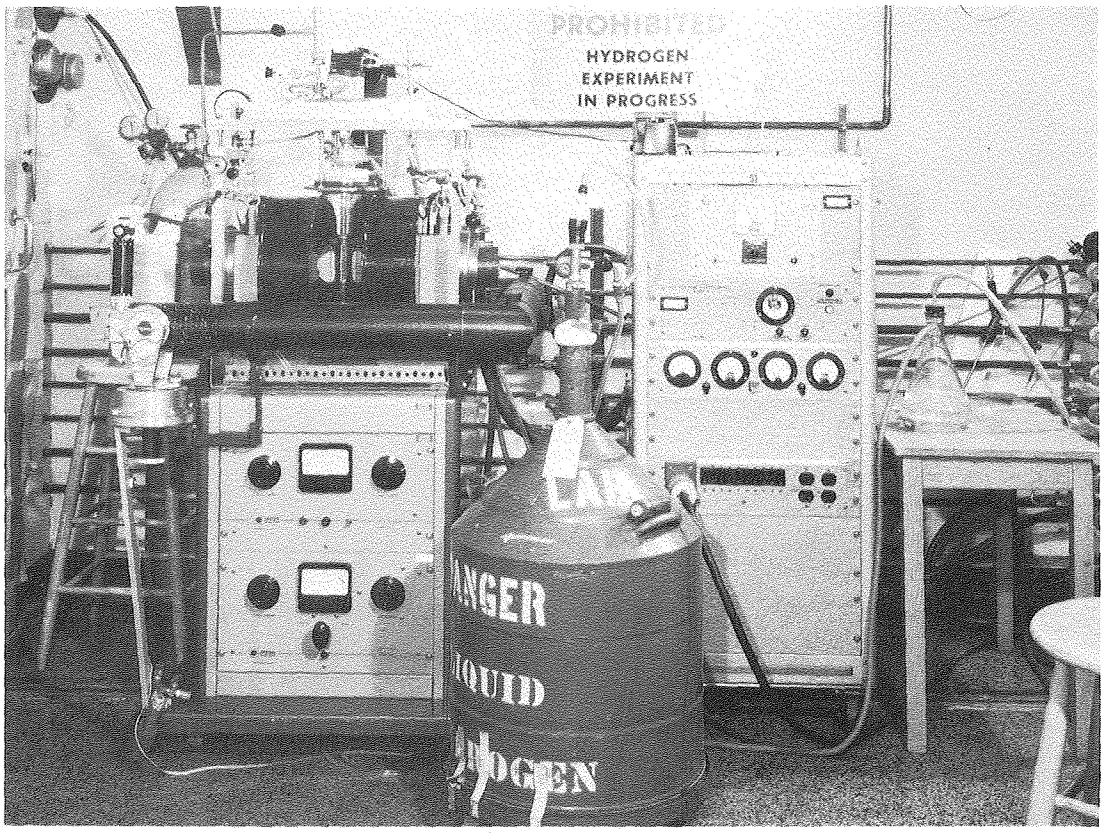

ZN-4958

Fig. 13. Low temperature apparatus.

is quite hard to use the same arrangement. Therefore, a three wall dewar[23] was used. The dewar bottom is the so-called three wall dewar, actually two walled with a copper finger acting as the third wall. This copper finger helps in cooling the lower part of the dewar to liquid nitrogen temperature when liquid nitrogen is added to the upper part. This will help in reducing the temperature gradient between the outer and inner dewar when the latter is filled with liquid hydrogen or helium. Hydrogen or helium is introduced into the inner dewar through a sealed, evacuated metal tube which goes about two inches inside the inner dewar. The whole assembly is connected to a brass head which has an opening serving as an outlet for the extra hydrogen or helium in the inner dewar. In this dewar arrangement, there is no quartz window at the bottom of the dewar. At first a dewar with a quartz window was tried at liquid helium temperature. It was very hard for light to pass through and therefore, it was very hard to see an image in the telescope. This was attributed to two factors, first, formation of a frost on the window and therefore, obstructing the light pass, second, vigorous boiling of the liquid due to the heat resulting from the light. Therefore, the present dewar without a window is used and the optical system was changed as will be seen below.

(3) Optical system. The optical system consists mainly of a telescope and a periscope. The Questar (a high resolution telescope available commercially) is used as a telescope. The minimum distance between the Questar and the object must be seven feet. The periscope was designed to maintain that distance at about nine feet. The periscope is made of aluminum tubes. The aluminum tubes are shaped in a form of a rectangle one side of which is raised to face the front surface mirror on which the light falls. The aluminum tubes are equipped with front surface mirrors to direct the light into the desired path. The light path starts from an ordinary microscope lamp, then through the inner tube by the aid of a front surface mirror, and then it is reflected from the bottom of the tube by the use of a gold reflector placed at the bottom. A tantalum reflector was tried first, but the image of the sample tube and the rest of the field

in the telescope were of the same color so that it was very hard to focus on the sample image. The focus and magnification are one of the major problems in this apparatus, making the magnitude of the experimental error higher than in the old apparatus.

(4) The inner tube. The quartz inner tube is not sealed to the dewar as in the other apparatus, but it is movable. It can be taken out of the inner dewar and put back easily. At the top of the inner tube is screwed a dural head which has a micrometer and a vacuum connection. The micrometer is used for measuring the deflection by the null method, and the vacuum connection for evacuating the inner tube. The whole inner tube assembly is screwed to the apparatus top.

2. Low temperature results.

The apparatus was calibrated as before using nickelous ammonium sulphate. The apparatus constants were calculated from the deflection at liquid nitrogen and liquid hydrogen temperatures.

The magnetic measurements were made on two old samples of curium metal (sample 3 and 6 in Table III). The measurements were carried out down to liquid hydrogen temperature. Some higher temperatures were tried to construct the $1/\chi$ vs T curve. The deflection obtained with the first sample was very small (within the experimental error, even smaller than the experimental error at most of the temperatures) due to the small weight of the sample and the small magnification of the new apparatus. The plot of $1/\chi$ vs. T for the second sample is shown in Fig. 14. The general behavior of the metal at high temperature is still clear from the straight line. However, due to the large experimental error it will be hard to calculate an accurate effective moment from this graph. The behavior of the metal at liquid nitrogen temperature is consistent with the results found already with the old apparatus. The result at liquid hydrogen temperature gives a magnetic susceptibility only slightly higher than at liquid nitrogen temperature. Perhaps a transition to an antiferromagnetic state occurs in this region.

With the present measurements it is very hard to reach any conclusion about the behavior of the metal at low temperature due to the large experimental error in the results. More accurate measurements at small temperature intervals are needed to detect any magnetic transition at low temperature.

B. Curium Trifluoride

The magnetic susceptibility of the rare earth metals is very similar to that of the +3 ions. Also the susceptibility calculated for a configuration of equivalent 4f electrons in the Russell - Saunders limit agrees quite well with these experimental results. For these reasons it is of interest to compare the susceptibility of curium metal with that of Cm III. Only one determination of the susceptibility of Cm^{+3} has been reported in the literature. Crane et al. measured the susceptibility of curium trifluoride at two temperatures.[4] Their results (corrected for diamagnetism of fluoride) are

$$\chi_{298^{o}} = 22{,}500 \pm 4000 \times 10^{-6} \text{ cgs}$$

$$\chi_{77^{o}K} = 58{,}000 \pm 6000 \times 10^{-6} \text{ cgs}$$

The limits of error in these measurements were rather large because of a combination of the use of small samples and the uncertainty of the temperature of the sample (due to the short half life of Cm^{242} which was used in those measurements).

In the work reported here the susceptibility of Cm^{+3} was determined in different curium compounds. The first of these conpounds is curium trifluoride. Curium trifluoride was chosen because, first it is non-hygroscopic and therefore it is easy to handle, second, it is the material used to prepare the metal and therefore, it will be good for comparison between the metal and the +3 ions.

The susceptibility of three samples of curium trifluoride was measured. Those samples are from different preparations used for producing the metal. Fluoride from these precipitations had been used

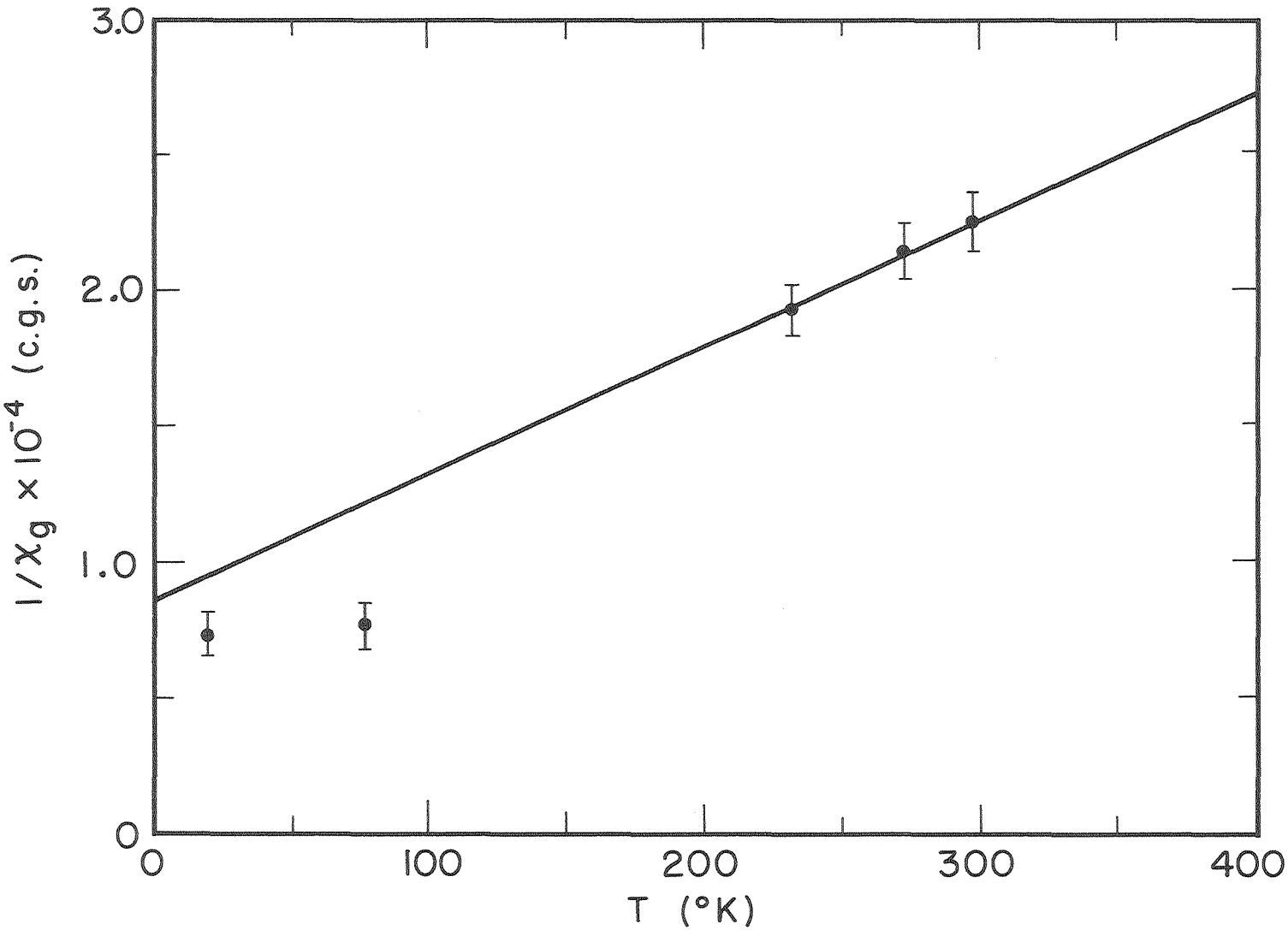

MUB-5766

Fig. 14. $1/\chi_g$ vs T(°K) for curium metal. (Sample 6)

in successful preparations of pure metals; the success indicated that there were no gross impurities present.

Measurements of the susceptibility were carried out in the temperature range of 77-300°K. The results of these measurements are given in tables 13-15. The reciprocal of the susceptibility was plotted vs the absolute temperature and the results are shown in Figs. 15-17. The susceptibility follows Curie-Weiss law over the whole range of temperature investigated. The Δ values calculated using an IBM 7094 computer least square fit program, are smaller than those of the metal. This is expected because the fluoride is much more magnetically dilute than the metal. Gadolinium has the same behavior as found in curium. The Δ values calculated for different samples range from 4-7°.

The effective moment calculated from different samples (using the molecular weight of $CmF_3 \cdot 1/2\ H_2O$) was found to be 7.71 ± 0.1. From the effective moment the g value can be calculated using the formula

$$u_{eff} = g\sqrt{J\ (J+1)}$$

The calculated g value was found to be 1.94 ± 0.03. This indicates that we do not have pure Russell-Saunders coupling.

C. Curium Oxychloride

Curium oxychloride was chosen to calculate the susceptibility of Cm^{+3} from another compound in which the surroundings of Cm^{+3} are different. The curium oxychloride used for measurements is presumably pure, since all the materials used in its preparation were checked for impurities. The curium oxychloride itself was identified by X-ray diffraction pattern.

The results of the measurements on CmOCl are shown in Tables XVI and XVII. The plots of the reciprocal of the susceptibility vs the absolute temperature are shown in Figs. 18 and 19. The susceptibility follows Curie-Weiss law over the range of temperature measured. The Δ values calculated for the two samples varies from 21 to 24°. The

Table XIII. Susceptibility of curium trifluoride (sample 1)

$T^{o}C$	$\chi \times 10^{6}$	$1/\chi\ 10^{-4}$
- 196	283.2 ± 1.0	0.353
- 75	110.5 ± 1.0	0.905
- 40.8	96.75 ± 1.0	1.034
0	83.25 ± 1.0	1.201
25	76.5 ± 1.0	1.307

$\Delta = 7^{o}$

$u_{eff} = 7.62 \pm 0.1$

$g = 1.92 \pm 0.02$

Table XIV. Susceptibility of curium trifluoride (sample 2)

$T^{o}C$	$\chi \times 10^{6}$	$1/\chi\ 10^{-4}$
- 196	299.26 ± 1.0	0.334
- 128	163.17 ± 1.0	0.613
- 75	124.01 ± 1.0	0.806
- 40.8	105.13 ± 1.0	0.951
0	88.21 ± 1.0	1.134
25	81.87 ± 1.0	1.221
$\Delta = 5^{o}$	u_{eff} = 7.87 ± 0.1	g = 1.98 ± 0.02

Table XV. Susceptibility of curium trifluoride (sample 3)

$T^{o}C$	$\chi \times 10^{6}$	$1/\chi\ 10^{-4}$
- 196	279.51 ± 1.0	0.358
- 128	155.58 ± 1.0	0.643
- 75	117.23 ± 1.0	0.853
- 40.8	98.66 ± 1.0	1.014
0	81.90 ± 1.0	1.221
25	77.44 ± 1.0	1.291
$\Delta = 4$	$u_{eff} = 7.63 \pm 0.1$	$g = 1.92 \pm 0.02$

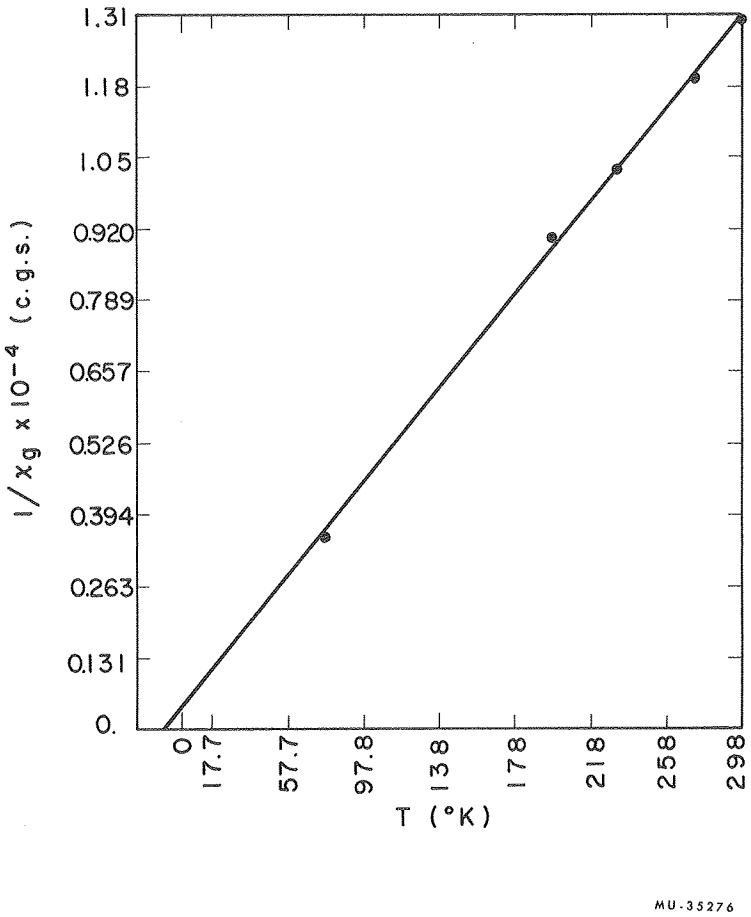

Fig. 15. $1/\chi_g$ vs T(^{o}K) for CmF_3. (Sample 1)

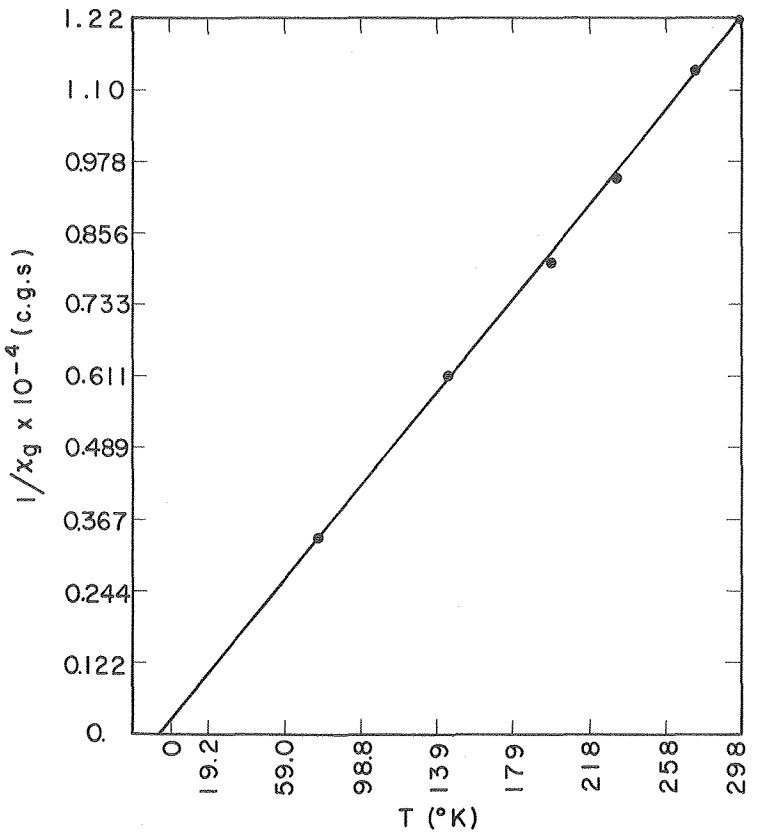

MU-35277

Fig. 16. $1/\chi_g$ vs T(^{o}K) for CmF_3. (Sample 2)

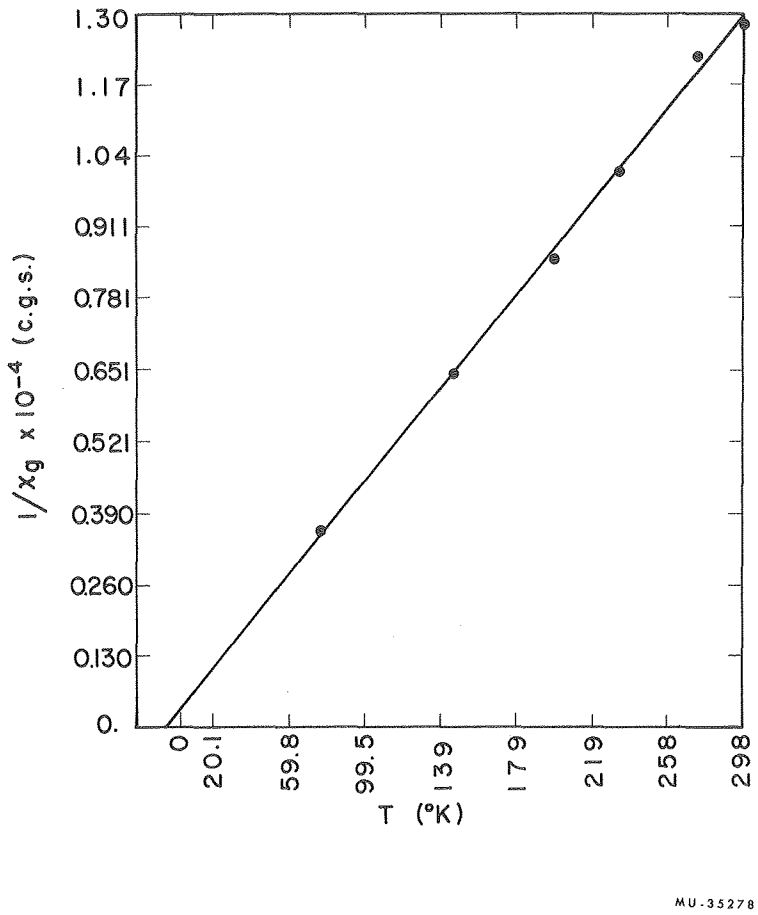

Fig. 17. $1/\chi_g$ vs T(°K) for CmF_3. (Sample 3)

effective moment calculated was found to be 7.58 ± 0.1 B.m. giving g value 1.91 ± 0.03. This value agrees within the experimental error with that obtained from the curium trifluoride.

D. Curium-lanthanum mixture

Delta, or the molecular field constant, may arise from three sources. First, Δ may appear as an empirical constant from the fact that the multiplet intervals are neither very large nor very small compared with kT. In this case the Curie constant, C, will itself change with temperature, and Δ will have no real significance and probably will not remain constant over a very large temperature interval. Gadolinium and presumably curium ions are in the S state and therefore, we are not bothered with multiplet structure.

The second source of the molecular-field constant is the effect of inhomogeneous electric fields produced by neighboring ions or oriented solvent dipoles on the orbital moment of the 4f electrons.

The third, and final source of Δ lies in the Heisenberg exchange interaction. When magnetic atoms or ions are very close together, this interaction has the effect of introducing a very strong coupling between the respective spins.

For gadolinium there is no multiplet structure so that Δ must here be due solely to exchange forces. Therefore, Δ will decrease with increase of magnetic dilution. The following table shows this behavior for some of gadolinium compounds[21]

Compound	$\Delta^{o}C$
Gd_2O_3	18 ± 2
$GdCl_3$	14
$Gd_2(SO_4) \cdot 8\ H_2O$	2 (or zero)

The order of compounds written down is almost certainly the order of increasing magnetic dilution, that is, the Gd^{+3} ions are getting farther

Table XVI. Susceptibility of curium oxychloride (sample 1).

$T^{o}C$	$\chi \times 10^{6}$	$1/\chi\ 10^{-4}$
-196	241.19 ± 1.0	0.415
-128	142.75 ± 1.0	0.701
- 75	109.19 ± 1.0	0.916
- 40.8	93.16 ± 1.0	1.073
0	80.34 ± 1.0	1.245
25	74.36 ± 1.0	1.345
$\Delta = 21^{o}$	$u_{eff} = 7.53 \pm 0.1$	$g = 1.90 \pm 0.02$

Table XVII. Susceptibility of curium oxychloride (sample 2).

$T^{o}C$	$\chi \times 10^{6}$	$1/\chi\ 10^{-4}$
-196	235.53 ± 1.0	0.424
- 75	110.59 ± 1.0	0.904
- 40.8	95.78 ± 1.0	1.044
0	80.82 ± 1.0	1.237
25	75.14 ± 1.0	1.331
$\Delta = 24^{o}$	$u_{eff} = 7.62 \pm 0.1$	$g = 1.92 \pm 0.02$

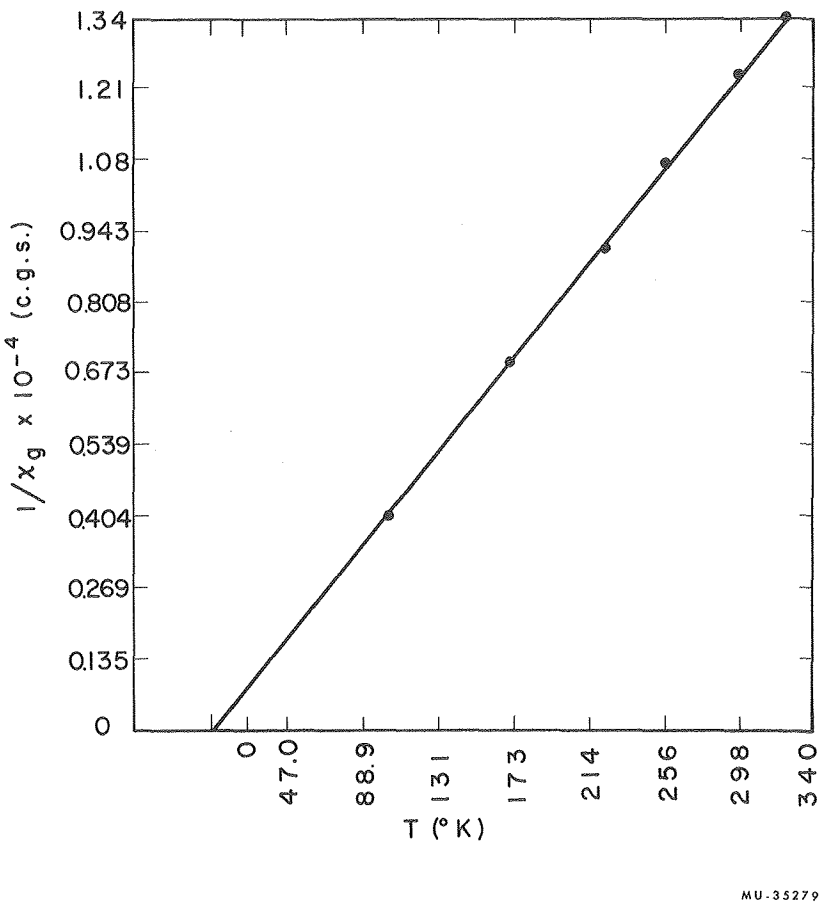

Fig. 18. $1/\chi_g$ vs T(^{o}K) for CmOCl. (Sample 1)

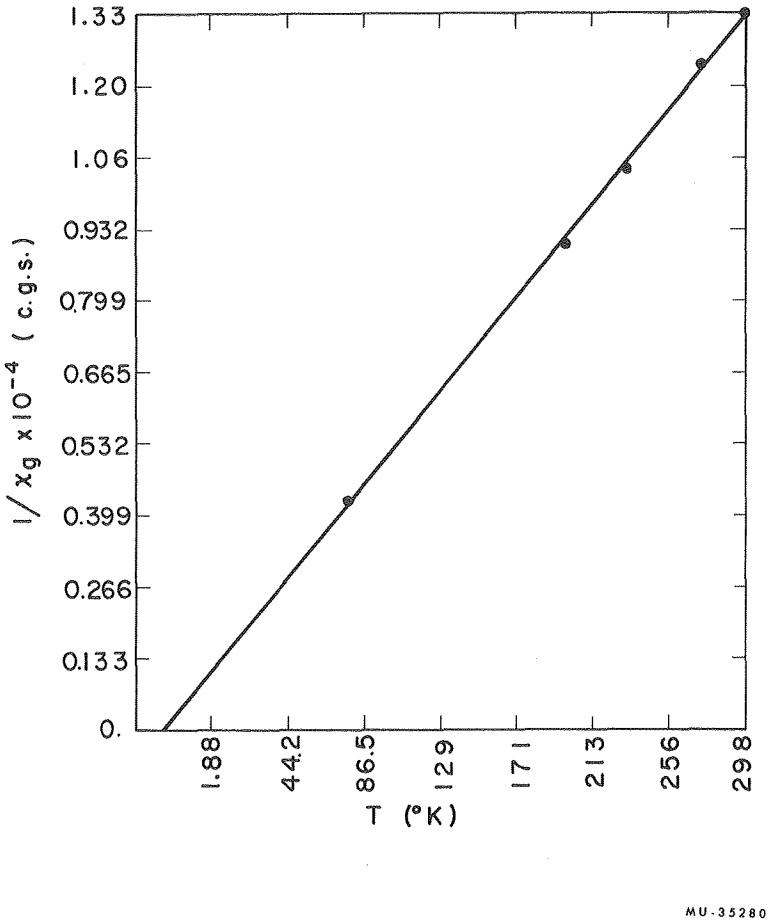

Fig. 19. $1/\chi_g$ vs T(^{o}K) for CmOCl. (Sample 2)

apart. It is therefore gratifying to see Δ decreasing until, in the octa hydrated sulphate, the exchange forces are presumably negligible.

With this in mind and due to the fact that curium presumably occupies the same place in the actinide series as gadolinium does in the lanthanides the diluted curium trifluoride with lanthanum matrix was measured. The measurements of two samples of 5.6 mole% curium in lanthanum matrix were carried out. The results obtained are shown in Tables XVIII and XIX. The values in the tables were corrected for the diamagnetism of lanthanum trifluoride which was determined experimentally in a separate experiment. The plot of the reciprocal of the susceptibility vs the absolute temperature are shown in Figs. 20 and 21. The Δ values obtained are quite small reaching the value of 4°, showing that the molecular field constant arises mainly from the magnetic interaction as in the case of gadolium. The Δ value obtained here is very close to that obtained in case of pure CmF_3.

The effective moments calculated for the two samples give $u_{eff} = 7.72 \pm 0.15$. This gives $g = 1.94 \pm 0.04$.

Table XVIII. Susceptilibity of curium trifluoride in lanthanum trifluoride matrix (sample 2).

$T^{o}C$	$\chi \times 10^{6}$	$1/\chi\ 10^{-4}$
-196	301.15 ± 4.0	0.322
- 75	114.37 ± 4.0	0.874
- 40.8	99.75 ± 4.0	1.002
0	85.18 ± 4.0	1.174
25	81.61 ± 4.0	1.225
$\Delta = 7.5^{o}$	$u_{eff} = 7.66 \pm 0.15$	$g = 1.93 \pm 0.04$

Table XIX. Susceptibility of curium trifluoride in lanthanum trifluoride matrix (sample 2).

$T^{o}C$	$\chi \times 10^{6}$	$1/\chi\ 10^{-4}$
-196	309.82 ± 2.5	0.316
- 75	124.95 ± 2.5	0.841
- 40.8	105.74 ± 2.5	0.966
0	88.92 ± 2.5	1.166
25	84.26 ± 2.5	1.184
$\Delta = 4^{o}$	$u_{eff} = 7.78 \pm 0.15$	$g = 1.96 \pm 0.04$

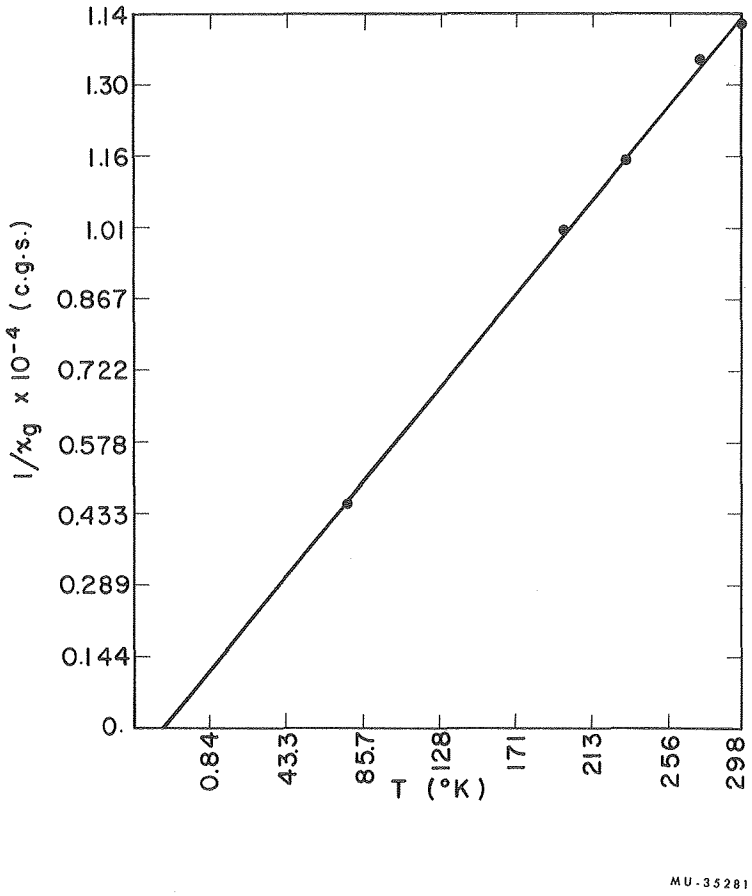

Fig. 20. $1/\chi_g$ vs T(°K) for CmF_3 (diluted with LaF_3 matrix). (Sample 1)

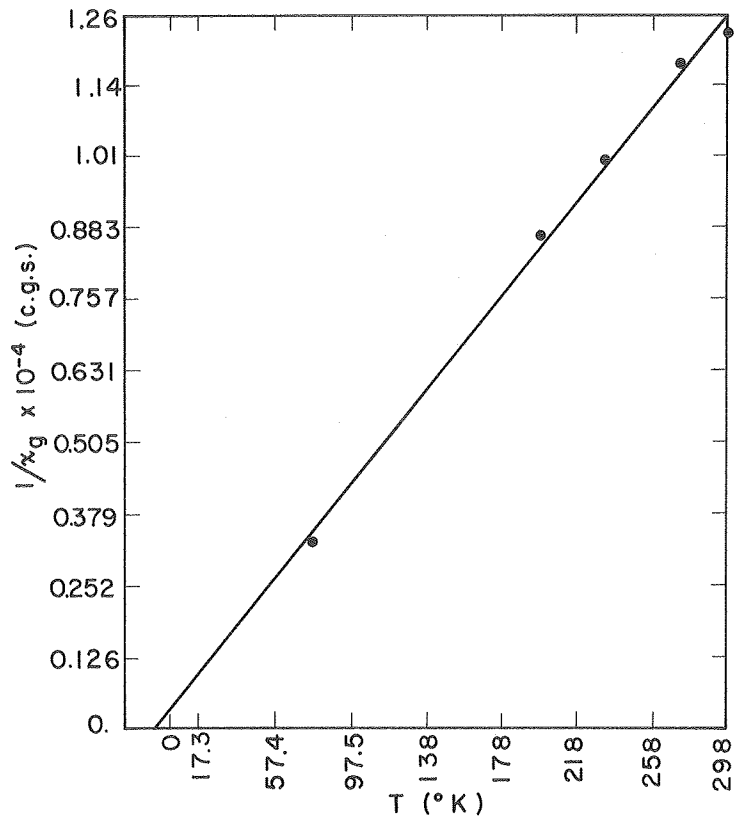

Fig. 21. $1/\chi_g$ vs T(^{o}K) for CmF_3 (diluted with LaF_3 matrix). (Sample 1)

VI. DISCUSSION

The magnetic susceptibility of curium metal presented above is markedly different from those of the preceding elements in the actinide series. This is true too with respect to the other physical properties known of curium. For example the melting point of curium is 345° higher than that of americium the preceding element in the actinide series. Curium has a close-packed structure[3] similar to that of americium and the early members of the rare-earth series. Plutonium has more allotropic forms and some of the phases have very complex structure, as do some of the phases of the two preceding elements, neptunium and uranium. The abrupt change in crystal structure of the actinides at americium and curium is illustrated in Fig. 22. The comparison of the magnetic properties of curium metal with the other actinide elements is shown in Fig. 23.

In the same figure the magnetic properties of the actinide metals are compared with those of the lanthanides and the second and third transition series elements.[22,24,25,26] The atomic volumes and the melting points of the actinide metals are compared with those of the lanthanides and the second and third transition series[2,25,26] in Fig. 24. These graphs show that actinium, americium, and curium are very similar to the rare-earth elements but that thorium, protactinium, uranium, neptunium, and plutonium have properties which are intermediate between those of the lanthanide and d transition series. The unusual crystal structure and magnetic properties of these elements indicate that they are really unique in the periodic table and there is little justification in classifying them simply as f or d transition elements.

The susceptibility change of curium metal with temperature above 77°K is very similar to that of gadolinium above room temperature. The metal follows Curie-Weiss law over the entire temperature range above 77°K, with a large Δ value (348° compared to -310° for Gd). Although the Δ value is large, and consequently the meaning of Curie-Weiss law is not very clear, the effective moment found is remarkably close to the theoretical value of the gaseous ions of $5f^7$ electrons. The value of the

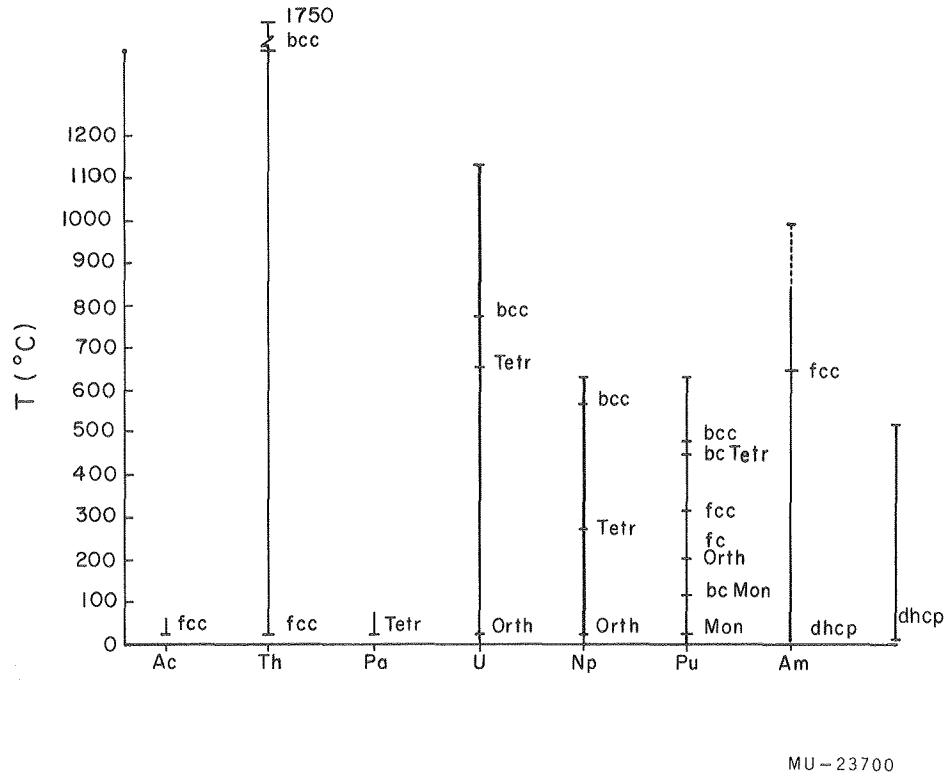

Fig. 22. Crystal structures of the actinide metals.

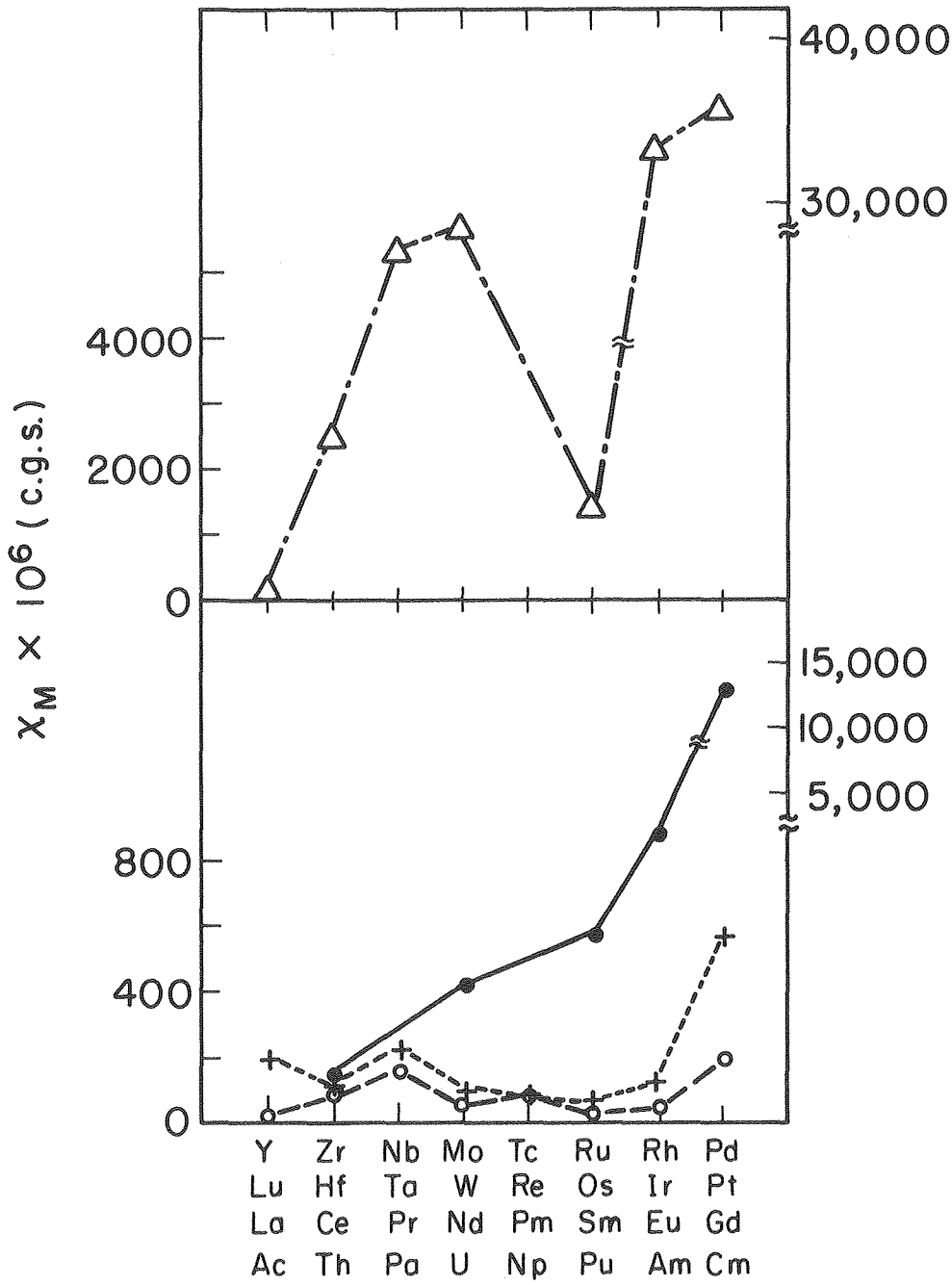

MUB-5765

Fig. 23. Magnetic proporties of "d" and "f" transition elements.
+-------+ Y, Zr, Nb ------ 4d transition series
o - - - o Lu, Hf, Ta ------ 5d transition series
Δ -.-.-.Δ La, Ce, Pr ------ 4f transition series
●———● Ac, Th, Pa ------ 5f transition series

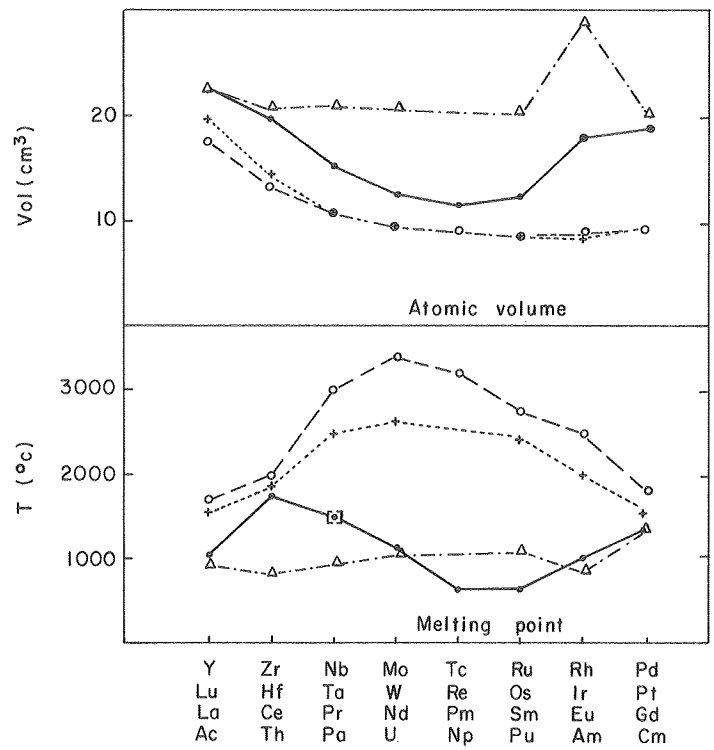

MU-23701

Fig. 24. Comparison of various properties of the transition elements, lanthanides, and actinides.

+.....+ Y, Zr, Nb .... 4d transition series

o --- o Lu, Hf, Ta .... 5d transition series

△ -.-.△ La, Ce, Pr .... lanthanide series

●——● Ac, Th, Pa .... actinide series

effective moment of 7.99 ± 0.15 is also in a very good agreement with the value of 8.07 ± 0.05 found recently for gadolinium.[22]

One other striking feature between curium and gadolinium is the large value of Δ in the metal and the decrease of this value with increasing dilution of the magnetic ions in the compound. This can be shown by comparing the results presented for curium with some of the results found about gadolinium.

Compound	Δ	Compound	Δ
Gd_2O_3	18 ± 2	CmOCl	24 ± 3
$GdCl_3$	14	$CmF_3 \cdot \frac{1}{2}H_2O$	5 ± 3
$Gd(SO_4)_3 \cdot 8H_2O$	2 (or zero)	$(Cm\text{-}La)F_3$	5 ± 3

The order of the compounds written is almost certainly the order of increasing "magnetic dilution" that is Gd^{+3} or Cm^{+3} are getting farther apart. Gadolinium is the only element in which this value approaches zero because Δ arises solely from the Heisenberg exchange interaction due to the presence of gadolinium in the S state. The same trend is very clear in curium indicating that the ground state of curium is mainly an S state.

The behaviour of curium metal at lower temperature is rather strange. However, extensive studies at low temperatures are needed before reaching any conclusion about the state of the metal at these low temperatures. Possibly there is a phase transition or a structure change at low temperature. The absence of ferromagnetism in double hexagonal curium at the temperature range studied is consistent with its absence in all the rare-earth metals which crystallize in this same structure. The departure of the metal from Curie-Weiss law at 77°K and its deviation toward ferromagnetism is very clear in all the measurements. However, the crystal structure of the metal at this temperature is very important to decide about the exact behaviour of the metal.

The work presented here indicates that curium metal is similar to the rare-earth metals in its properties. Americium metal was found before to be a rare-earth-like metal.[1]

Qualitatively, therefore, the complex nature of the early actinide metals can be understood by considering the electronic configuration of the gaseous atoms of the actinides and lanthanides as determined by atomic beam resonance studies. These are presented in Table XX.[27] (The configurations show the electrons above the radon and xenon cores respectively.) The 6d electrons are bound more tightly than the 5f electrons, and, as a result of this, there is a d electron in the gaseous atoms up to plutonium. The relative binding energies of the last competing electron in the lanthanides and the actinides are presented in Fig. 25 (taken from Cabezas[28]). In the lanthanide elements the f band is lower in energy and more internal thus leading to normal physical properties and simple crystal structures. In the actinides the d and f bands are very close in energy and probably overlap, giving rise to a much more complicated electronic structure which is the cause of the abnormal physical properties and the complex crystal structures observed between protactinium and plutonium. This also leads to more than the "normal" three bonding electrons which probably accounts for the smaller atomic volumes and high heats of vaporization in this region of the periodic table.

The results presented here about curium ion in various curium compounds support the actinide concept and show the departure from Russell-Saunders coupling in the actinide elements. In the rare-earth region the susceptibility calculated from the Van Vleck formula[29] for a configuration of equivalent 4f electrons in Russell-Saunders coupling agrees very well with the experimental results. There are three cases, however, to be considered:

(a) Multiplet intervals large compared to kT

$$\chi_M = \frac{N g^2 \beta^2 J(J+1)}{3kT} + N\alpha$$

Table XX. Electronic configuration of the gaseous atoms of the actinide and lanthanide elements (Ref. 27).

Actinide elements	Configuration	Lanthanide elements	Configuration
Ac	$6d7s^2$	La	$5d6s^2$
Th	$6d^2 7s^2$	Ce	$(4f5d6s^2)$
Pa	$5f^2 6d7s^2$	Pr	$4f^3 6s^2$
U	$5f^3 6d7s^2$	Nd	$4f^4 6s^2$
Np	$5f^4 6d7s^2$	Pm	$4f^5 6s^2$
Pu	$5f^6 7s^2$	Sm	$4f^6 6s^2$
Am	$5f^7 7s^2$	Eu	$4f^7 6s^2$
Cm	$5f^7 6d7s^2$	Gd	$4f^7 5d6s^2$

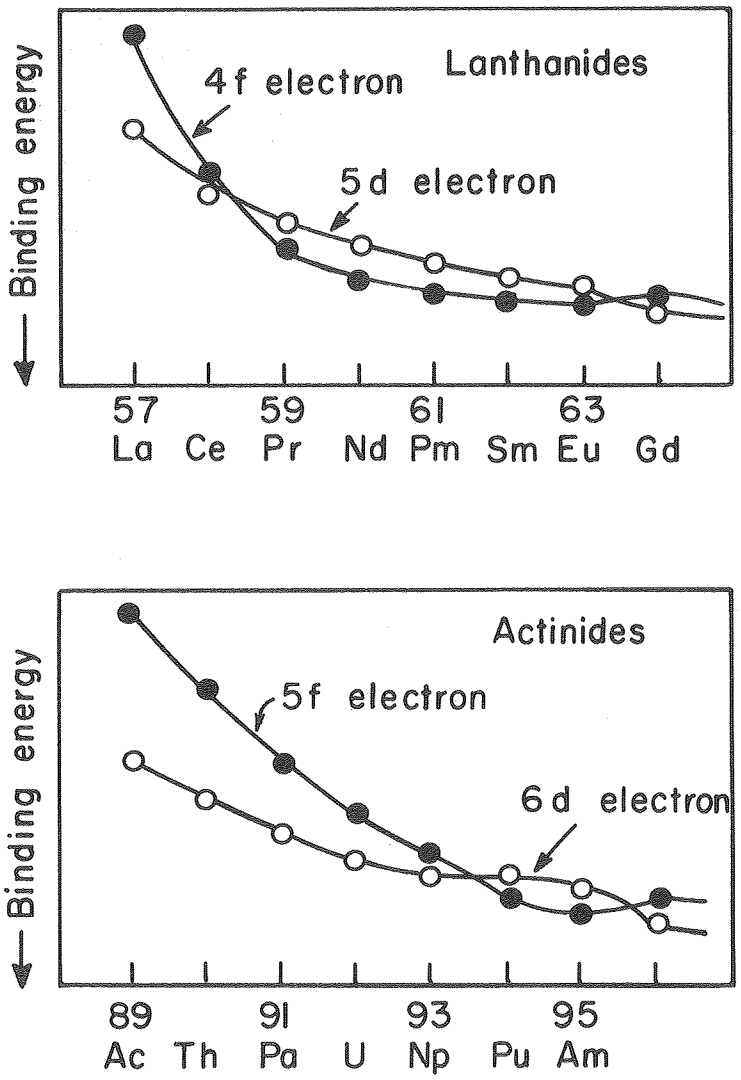

MU-23703

Fig. 25. Qualitative comparisons of the binding energies of the last competing electron in the lanthanides and actinides.

where

$$g = \text{Landé splitting factor}$$

$$= 1 + \frac{S(S+1) + J(J+1) - L(L+1)}{2J(J+1)}$$

J is the vector sum of S and L (the resultant spin and orbital angular momentum of the atom respectively). $N\alpha$ is the high frequency term, or temperature independent term due to second order Zeeman effect

$$= \frac{N\beta^2}{6(2J+1)} \left[\frac{F(J+1)}{h\nu(J+1;J)} - \frac{F(J)}{h\nu(J;J-1)} \right]$$

$$F(J) = \frac{1}{J} \left[(S + L + 1)^2 - J^2 \right] \left[J^2 - (S - L)^2 \right]$$

(b) Multiplet intervals small compared to kT: In this case the high frequency term is absent (neglecting the diamagnetic term). The susceptibility arises solely from the low frequency part. Therefore the susceptibility can be expressed by the formula

$$\chi_M = \frac{N\beta^2}{3kT} \left[4S(S+1) + L(L+1) \right]$$

(c) Multiplet intervals comparable to kT: This is the general case from which the previous two limiting cases can be derived easily. It involves the summation of the contribution of atoms with different values of J. The number N_J, is determined by Boltzmann temperature factor:

$$\chi_M = \frac{N \sum_{L-S}^{L+S} \left[g_J^2 \beta^2 J(J+1)/3\, kT + \alpha_J \right] (2J+1)\, e^{-W_J^o/kT}}{\sum_J (2J+1)\, e^{-W_J^o/kT}}$$

The function g_J and α_J (with the same definition as in (a)) are derived from the matrix elements $\langle JM|L_z + 2S_z|J'M'\rangle$. The spin-orbit coupling which splits the LS terms into J levels also couples together states of the same J but different S and L, causing departure from Russell-Saunders coupling.[30]

The gaseous ions of most of the rare-earth elements follow the equation of (a) above where the multiplet intervals are large compared to kT. In the case of gadolinium (and presumably curium) which has a $^8S_{7/2}$ ground state and where there is no multiplet structure the high frequency term of the equation of (a) will be equal to zero (because S-L = J and therefore F(J) = 0). The formula in (a) will take the form

$$\chi_M = \frac{N g^2 \beta^2 J(J+1)}{3kT}$$

For a ground state $^8S_{7/2}$ in Russell-Saunders approximation the g value will be equal 2.0. The spin-orbit coupling parameters of the actinides are approximately twice as large, and the electrostatic parameters two thirds as large, as those of the corresponding lanthanides.[31] As a result, the energy level structures of the actinides exhibit considerable departure from Russell-Saunders coupling. Consequently, due to the mixing of the ground state with the states of the same J values because of the large spin-orbit coupling constant, the g value in curium is expected to be smaller than that in gadolinium. The value of g found here for the curium ion in different curium compounds is equal to 1.93 ± 0.03. This value is in good agreement with the value found by Marvin Abraham et al. by measuring the paramagnetic resonance spectrum of Cm^{+3} substituted in small amounts for La^{+3} in lanthanum ethyl sulphate and lanthanum trichloride crystals.[32] The value found here is higher than that calculated by Wybourne[31] by assuming 5f hydrogenic ratios for the Slater integrals F_2, F_4, and F_6. The best fit to the solution spectra of Cm^{+3} in 1.0 M $HClO_4$ was obtained with $|X| = \xi/F_2 = 10.6$ and $F_2 = 280\ cm^{-1}$, where ξ is the spin-orbit coupling constant. The agreement, however, was not very good. Conway[33] has calculated the eigen values, the eigen vectors, and

the g values corresponding to different values of the parameter $|X|$. From the graph of g vs $|X|$ constructed from Conway's calculation the value of g presented here would correspond to $|X|$ of 11. This $|X|$ value would correspond to an eigen vector of the ground state of curium ion of the form

$$0.921|^8S\rangle + 0.3659|^6P\rangle - 0.067|^6D\rangle + 0.0135|^6F\rangle$$

For comparison the ground-state eigen vector of gadolinium ion was found to be[31]

$$0.9844|^8S\rangle + 0.1736|^6P\rangle - 0.140|^6D\rangle .$$

The results presented here together with those obtained from paramagnetic resonance on single crystals show that there is a considerable departure from Russell-Saunders coupling with a pronounced tendency toward jj coupling in the actinide region. The actual coupling will be intermediate between the two.

From the results presented above about the magnetic susceptibility of curium ion in several curium compounds it is clear that curium has the same configuration as gadolinium. This would be supported by the comparison of the magnetic susceptibility of the actinide ions with those of the lanthanide ions. This comparison is shown in Fig. 26.[2,34]

The qualitative similarity of the actinide curve to the lanthanide can be interpreted as evidence for $5f^n$ electron configuration for the magnetic electrons in the actinide series. The fact that the experimental magnetic moments are generally lower than the theoretical values can be interpreted as resulting from a Stark effect produced by electric fields of anions or water dipoles in case of solutions. This effect will be more pronounced in the case of 5f than in the 4f because there is less electrostatic shielding by outer electrons of 5f than 4f electrons. Partial failure of the Russell-Saunders approximation could also account for some of the discrepancy. This was clearly discussed in the case of curium with the results presented in this work.

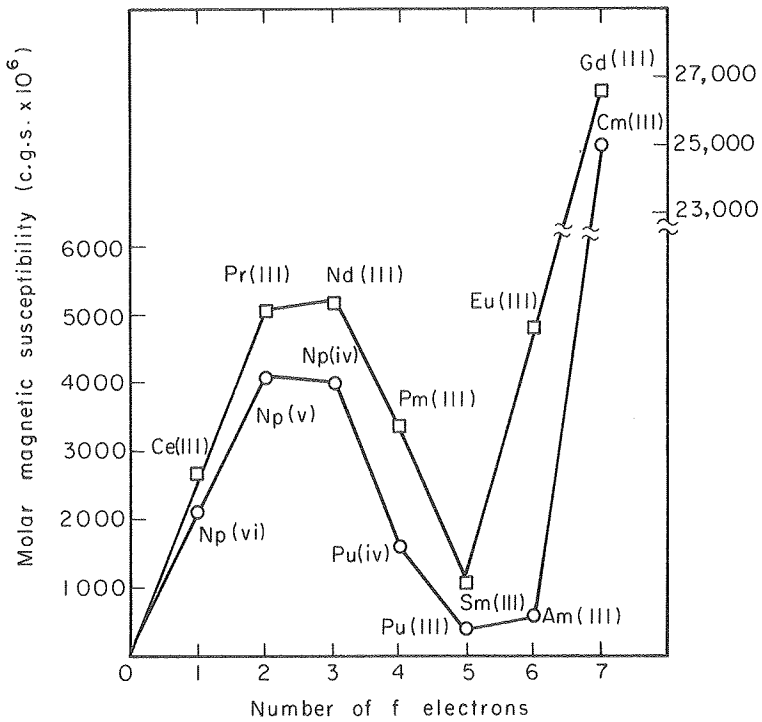

MU-35283

Fig. 26. Molar magnetic susceptibility of some actinide and lanthanide ions.

Selwood[21] has challenged the conclusion about the similarity of the actinide and lanthanide curves. He has pointed out that by selecting certain magnetic susceptibility data and excluding others a curve showing two maxima can be constructed for several elements of the first transition series which resembles that shown in Fig. 26 for actinide and lanthanide elements. Since no f electrons are present in the first transition series, this challenges the validity of the analogy between lanthanide and actinide elements derived from Fig. 26. The construction of this Selwood curve is, however, extremely enlightening, for it shows that even by selecting anomalous cases and special conditions, presumably in order to make it resemble as much as possible Fig. 26, the basic difference in the magnetic behaviour of d and f electrons cannot be erased. For example, the susceptibility of Fe III in dilute aqueous solution at pH 2 is $\approx 6600 \times 10^{-6}$ c.g.s. units. This value is close to the spin only value for 5 unpaired electrons and shows that the magnetic electrons in Fe III are 3d electrons. The susceptibility of Pu III and Sm III on the other hand are quite small ($\approx 1000 \times 10^{-6}$ c.g.s.) and can only be interpreted on the basis of 5 unpaired f electrons. Similarly, Crane, Wallmann, and Cunningham[4] and later McWhan[2] made magnetic measurements of AmF_3 and obtained for the molar susceptibility 566×10^{-6} and 848×10^{-6} c.g.s. at 295 and 77°K, respectively. Here also the values obtained are much smaller than for the first transition series.

For ions with 5 and 6 unpaired electrons the multiplet intervals are not large compared to kT, and the general formula in Sec. (c) must be used to calculate the susceptibilities. This calculation was done by Van Vleck and Frank[35] in the case of samarium and europium and the discrepancy between the theoretical and experimental values was resolved. In the case of plutonium III and americium III McWhan[2] calculated the susceptibilities using the general formula in Sec. (c) and taking into account the departure from Russell-Saunders coupling. He obtained values agreeing with the experimental results. From Van Vleck's calculations, the susceptilibity of samarium should pass through a temperature minimum in the neighborhood of 400°K; such a minimum has in fact been observed

experimentally. Elliott and Lewis[36] made measurements on PuF_3 and $Pu_2(C_2O_4)_3 \cdot 9H_2O$ from 76 to 300°K. Dawson, Mandleberg, and Davies[37] extended measurements on PuF_3 and $PuCl_3$ up to about 600°K and found a minimum in the susceptibility-temperature curve at about 500 to 555 K. This is a good qualitative evidence that plutonium III has the electronic configuration $5f^5$.

Susceptibility measurements have been made on a large number of uranium (IV) compounds by many authors.[38-52] The results lie in the range of 3200 to 3800 × 10^{-6} c.g.s. units (at room temperature) which is closer to the $6d^2$ spin only value of 3333 than to the limiting $5f^2$ value of 5390, although a number of these investigators have interpreted their experimental results in terms of $5f^2$ configuration. However, paramagnetic exchange interaction (Δ) may be the reason for the low values. This is supported by the results of Hutchinson and Elliott[38] where the Weiss constant for uranium sulphate, oxalate and acetyl acetonate are found to be 113°, 168°, and 101°, respectively. The measurements of P. Handler and C. A. Hutchinson, Jr.[53] on uranium trichloride diluted with isomorphous diamagnetic lanthanum trichloride also support this conclusion. It was found that the values for uranium trichloride at infinite dilution are very similar to those of $Nd(C_2H_5SO_4)_3 \cdot 9H_2O$. Dawson[54] also made measurements on plutonium tetrafluoride and plutonium dioxide diluted with the isostructural diamagnetic compounds thorium tetrafluoride and thorium dioxide, respectively. The magnetic susceptibilities were found to increase with dilution, and the extrapolated values at infinite dilution for room temperature (3020 × 10^{-6} c.g.s. units) correspond essentially to the value predicted (3010 × 10^{-6} c.g.s. units) for the configuration $5f^4$.

Several measurements and theoretical analyses[55-60] have been made on compounds containing NpO_2^{+2} and NpO_2^{-1} ions. The results confirm the presence of one f and two f electrons, respectively.

From the results presented above, and the survey of the magnetic measurements made on the actinides, the indicated number of 5f electrons are present in the following ions
$Cm^{+3}(5f^7)$, $Am^{+3}(5f^6)$, $Pu^{+3}(5f^5)$, $Pu^{IV}(5f^4)$, NpO_2^{+}, $PuO_2^{+2}(5f^2)$, $NpO_2^{+2}(5f^1)$,

ACKNOWLEDGMENTS

It is a pleasure for me to express my thanks to Professor Burris B. Cunningham. His constant presence and willingness to help have provided encouragement, and his suggestions invariably have pointed to the core of the problem.

I wish to thank Dr. James Wallmann; without his help with experimental problems and his moral support this work would not have been completed.

My deep thanks to Mr. Tom Parsons whose help and encouragement will never be forgotten. His designing and building of the low temperature apparatus opened the way for low temperature measurements.

A special vote of thanks is given to Mr. Brij M. Bansal for his help in most of the experimental measurements and for his useful suggestions. I wish to thank Dr. Katheryn R. Rajnak for her valuable suggestions and for helping me in many of the theoretical problems.

I would like to thank Mr. George Shalimoff for making the spectrographic analyses. I would like to thank also Dr. John L. Burnett and Mr. Jere Green for their assistance and for our useful discussions.

The help in the laboratory of Miss Lilly Goda, Mrs. Lillian White, and Mrs. Gertrude Bolz, the health chemistry monitor, has been invaluable.

The greatest gratitude is due my wife, whose moral support, encouragement, and patience kept up my spirits and aided greatly on the road to a Ph.D. degree.

I would like to express my appreciation to the U.A.R. government for their support.

This work was done under the auspices of the U. S. Atomic Energy Commission.

$UO_2(5f^0)$, $U^{+3}(5f^3)$, and $U^{+4}(5f^2)$. The magnetic data obtained by Cunningham[6] on Bk^{+3} and Cf^{+3} indicate that the electronic configurations are $5f^8$ and $5f^9$, respectively. For Th^{+3} and Th^{+2} the evidence strongly favors a 6d assignment.[26]

These conclusions are consistent with many of the conclusions reached about the physical and chemical properties of the actinides, which also indicate that the 6d and 5f levels are of nearly equivalent energy in the first few elements of the series. The 5f electron levels lie lower once these elements are passed and the rare-earth-like properties predominate.

REFERENCES

1. D. B. McWhan, B. B. Cunningham, and J. C. Wallmann, J. Inorg. Nucl. Chem. 24, 1025 (1962).
2. D. B. McWhan (Ph.D. Thesis), University of California Lawrence Radiation Laboratory Report UCRL-9695, May 1961 (unpublished).
3. B. B. Cunningham and J. C. Wallmann, J. Inorg. Nucl. Chem. 26, 271 (1964).
4. W. W. Crane, J. C. Wallmann, and B. B. Cunningham, University of California Lawrence Radiation Laboratory Report UCRL-846, 1950 (unpublished).
5. W. W. Crane (Ph.D. Thesis), University of California Lawrence Radiation Laboratory Report UCRL-1220 (unpublished).
6. B. B. Cunningham, J. Chem. Ed. 36, 31 (1959).
7. P. Cosse, J. Inorg. Nucl. Chem. 14, 127 (1960).
8. L. Jackson, Phil. Trans. Roy. Soc. London A224, 1 (1924).
9. F. Trombe, Rev. Met. 52, 2 (1956).
10. S. Fried, E. F. Westrum, Jr., H. L. Baumback, and P. L. Kirk, J. Inorg. Nucl. Chem. 5, 182 (1958).
11. J. C. Wallmann, W. T. Crane, and B. B. Cunningham, J. Am. Chem. Soc. 73, 493 (1951).
12. S. Fried and N. R. Davidson, J. Am. Chem. Soc. 70, 3539 (1948).
13. J. C. Wallmann and B. B. Cunningham, University of California Lawrence Radiation Laboratory Report UCRL-8369, July 1958 (unpublished).
14. S. G. Thompson and M. L. Muga, Proceedings of the 2nd International Conference on the Peaceful Uses of Atomic Energy, Geneva, 1958 (United Nations, Geneva, 1959), P/825.
15. B. B. Cunningham, Microchemical Journal Symposium Series, Vol. 1 Submicrogram Experimentation (Interscience, New York, 1961), p. 69.
16. J. K. Dawson and R. M. Elliott, AERE Report C/R 1207 (1953).
17. G. Foex, C. J. Corpter, and L. J. Smits, Constantes Slectionnees Diamagnetisme Et Paramagnetisme (1957).
18. A. C. Demildt, University of California Lawrence Radiation Laboratory Report UCRL-10324-Rev., 1963 (unpublished).

19. C. W. Koch (Ph.D. Thesis), University of California Lawrence Radiation Laboratory Report UCRL-2286, 1953 (unpublished).

20. International Critical Tables (McGraw-Hill Co., Inc., New York, 1926).

21. Pierce W. Selwood, Magneto Chemistry (Interscience Publishers, Inc., New York, 1956).

22. Eugene V. Kleber, Rare Earth Research (MacMillan Co., New York, 1961).

23. L. J. Schoem and H. P. Broida, Rev. Sci. Instr. 33, 470 (1962).

24. J. C. Kriessman and H. B. Callen, Phys. Rev. 94, 837 (1954).

25. K. A. G. Schneider, "Critical Review of the Alloy Systems of Rare Earth, Scandium, and Yttrium Metals, Preprint of AEC-LA Report.

26. J. J. Katz and G.T. Seaborg, The Chemistry of the Actinide Elements (Methuen and Co., London, 1957).

27. A. Y. Cabezas (Ph.D. Thesis), University of California Lawrence Radiation Laboratory Report UCRL-9346, August 1960 (unpublished) .

28. B.B.Cunningham, "Comparative Chemistry of the Lanthanide and Actinide Elements," Paper presented at the XVII International Congress of Pure and Applied Chemistry, Munich, 1959.

29. J. H. Van Vleck, "The Theory of Electric and Magnetic Susceptibilities," Oxford, 1932.

30. B. R. Judd and I. P. K. Lindgren, Phys. Rev. 122, 1802 (1961).

31. W. T. Carnall and B. G. Wybourne, J. Chem. Phys. 40, 3428 (1964).

32. M. Abraham, B. R. Judd, and H. H. Wickman, Phys. Rev. 130, 611 (1963).

33. J. G. Conway (Lawrence Radiation Laboratory), private communication.

34. J. J. Howlander, Jr. and M. Calvin, J. Chem. Phys. 18, 239 (1950).

35. J. H. Van Vleck and A. Frank, Phys. Rev. 34, 1494 (1929).

36. N. Elliott and W. B. Lewis, AECD-2910, 1950.

37. J. K. Dawson, C. J. Mandleberg, and D. Davies, J. Chem. Soc. 2047 (1951).

38. C. A. Hutchinson, Jr. and N. Elliott, J. Chem. Phys. 16, 920 (1948); Phys. Rev. 73, 1229 (1948).

39. J. K. Dawson and M. W. Lister, J. Chem. Soc. 2181 (1951).

40. W. Trzebiatowski and P. W. Selwood, J. Am. Chem. Soc. 72, 4505 (1950).
41. J. K. Dawson, J. Chem. Soc. 2889 (1951); 1185 (1952).
42. N. Elliott, Phys. Rev. 76, 431 (1949).
43. J. K. Dawson, J. Chem. Soc. 429 (1951).
44. L. Sacconi, Atti accad., naz. Lincei. 6, 639 (1949).
45. H. Haraldsen and R. Bakken, Naturwiss. 28, 127 (1940).
46. H. Bommer, Z. anorg. Chem. 247, 249 (1941).
47. N. Elliott, L. Corliss, and Y. Delabare, Brookhaven National Laboratory Report BNL-39 (AS-3), December 1949, p. 47.
48. R. Stoenner and N. Elliott, J. Chem. Phys. 19, 950 (1951).
49. N. Elliott and W. B. Lewis, U.S. Atomic Energy Commission Document, AECD-2910, 1950.
50. E. Slowinski and N. Elliott, Brookhaven National Laboratory Report BNL-1199.
51. J. K. Dawson and M. W. Lister, J. Chem. Soc. 5041 (1952).
52. C. A. Hutchinson, Jr. and C. M. Herzfeld, J. Chem. Phys. 23, 1650 (1955).
53. P. Handler and C. A. Hutchinson, Jr., J. Chem. Phys. 25, 1210 (1956).
54. J. K. Dawson, J. Chem. Soc. 1882 (1952).
55. D. M. Gruen, Argonne National Laboratory Report ANL-4469, June, 1950.
56. D. M. Gruen and C. A. Hutchinson, Jr., J. Chem. Phys. 22, 386 (1954).
57. R. J. Elliott, Phys. Rev. 89, 659 (1953).
58. J. C. Eisenstein and M. H. L. Pryce, Proc. Roy. Soc. (London) A229, 20 (1955); A238, 31 (1956).
59. J. K. Dawson, Nucleonics 10 39 (1952).
60. J. K. Dawson and G. R. Hall, Proceedings International Conference on the Peaceful Uses of Atomic Energy, Geneva, 1955 (United Nations, Geneva, 1956), P/440, p. 231.

This report was prepared as an account of Government sponsored work. Neither the United States, nor the Commission, nor any person acting on behalf of the Commission:

A. Makes any warranty or representation, expressed or implied, with respect to the accuracy, completeness, or usefulness of the information contained in this report, or that the use of any information, apparatus, method, or process disclosed in this report may not infringe privately owned rights; or

B. Assumes any liabilities with respect to the use of, or for damages resulting from the use of any information, apparatus, method, or process disclosed in this report.

As used in the above, "person acting on behalf of the Commission" includes any employee or contractor of the Commission, or employee of such contractor, to the extent that such employee or contractor of the Commission, or employee of such contractor prepares, disseminates, or provides access to, any information pursuant to his employment or contract with the Commission, or his employment with such contractor.